JACS
JOURNAL OF THE AMERICAN CHEMICAL SOCIETY
Article
pubs.acs.org/JACS

Thermodynamic and Kinetic Stabilities of Complementary Double Helices Utilizing Amidinium−Carboxylate Salt Bridges

Hidekazu Yamada, Zong-Quan Wu, Yoshio Furusho,† and Eiji Yashima*

Department of Molecular Design and Engineering, Graduate School of Engineering, Nagoya University, Chikusa-ku, Nagoya 464-8603, Japan

Supporting Information

ABSTRACT: A series of dimer strands consisting of *m*-terphenyl backbones bearing complementary chiral or achiral amidines and achiral carboxylic acid residues connected by various types of linkers, such as diacetylene, Pt(II)-acetylide, and *p*-diethynylbenzene linkages, were synthesized by a modular strategy, and their chiroptical properties on the complementary double helix formations were investigated by absorption, circular dichroism (CD), and ^{1}H NMR spectroscopies. The thermodynamic and kinetic stabilities of the complementary double helices assisted by amidinium−carboxylate salt bridges are highly dependent on their linkages, and the thermodynamic analyses of the dimer duplexes revealed that the association constants increased in the order: Pt(II)-acetylide linker < *p*-diethynylbenzene linker < diacetylene linker, which is in agreement with the reverse order of their bulkiness. The substituents on the amidine groups were also found to affect the stabilities on the duplexes and the association constants increased in the order: isopropyl < (*R*)-1-phenylethyl < cyclohexyl. In addition, the introduction of electron-donating and/or electron-withdrawing substituents at the phenyl groups of the *p*-diethynylbenzene linkers connecting the amidine and carboxylic acid units, respectively, tends to stabilize the complementary double helices, especially in polar solvents, such as DMSO, due to the attractive charge-transfer interactions between the aromatic linkers, although the salt bridge formation is hampered in DMSO. Furthermore, the kinetic analyses of the chain exchange reactions for the duplexes bearing diacetylene and *p*-diethynylbenzene linkages showed that these were slow processes with negative $\Delta S^{\ddagger}$ values, meaning that the chain exchange reactions proceed via direct exchange pathways. In contrast, those for the duplexes bearing Pt(II)-acetylide linkages were fast processes supported by positive $\Delta S^{\ddagger}$ values, suggesting that the chain exchange reactions proceed via dissociation−exchange ones. The helix-inversion kinetics investigated for the racemic dimer duplexes composed of achiral amidines based on variable-temperature ^{1}H NMR measurements indicated that the barriers for the helix-inversion increased in the order: Pt(II)-acetylide linker, *p*-diethynylbenzene linker < diacetylene linker.

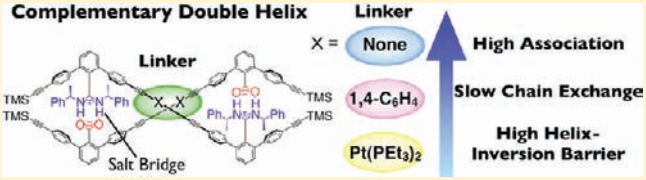

INTRODUCTION

Since the discovery of the α-helix in proteins[1] and double helix in DNA,[2] amazing strides have been made in molecular biology, and their sophisticated functions have been elucidated at a molecular level.[3] The discoveries of these biological helices with remarkable functions have also significantly stimulated chemists to challenge making artificial single- and double-stranded helical polymers and oligomers (foldamers), aiming mainly at mimicking such biological helical structures in the early stages and even now.[4] The one-handed helicity is specific to the DNA double helix and protein's α-helix because of the homochirality of their components, which is critical and of key importance for their remarkable functions. Currently, a number of synthetic polymers[4a,b,5] and oligomers[4c,6] with a controlled helical conformation have been reported, also for their applications in the development of unique chiral materials for separating enantiomers and asymmetric catalysis.[4a,5q] However, a limited number of structural motifs[7−11] are still available for constructing double helices except for the DNA analogues (peptide nucleic acids, PNA)[12] and the helicates,[7a−d,13] the metal coordination-driven helical assemblies.

A novel class of metal-free double-stranded helices has recently been reported by Lehn, Huc, and co-workers based on aromatic oligoamides that fold into double helices primarily through interstrand aromatic interactions along with hydrogen bondings.[8] Although such a hydrogen-bonding-driven self-assembly is a readily available and versatile approach to construct supramolecular duplexes, it remains difficult and challenging to design double helices on the basis of interstrand hydrogen-bonding, since most duplexes assembled via hydrogen-bonding interactions result in zipper or ladder structures.[14] The oligoresorcinols, types of *m*-phenylene oligomers, with specific chain lengths have also been found to self-assemble into well-defined double-stranded helical structures in water through interstrand aromatic interactions.[9] These double helices are unique and promising for further research and development of double helices with specific functions, but most of the double helices reported to date lack the important key feature of DNA, that is, the complementarity of the strands.[8e,11d,15]

Received: April 17, 2012
Published: May 8, 2012

 © 2012 American Chemical Society dx.doi.org/10.1021/ja303701d | J. Am. Chem. Soc. 2012, 134, 9506−9520

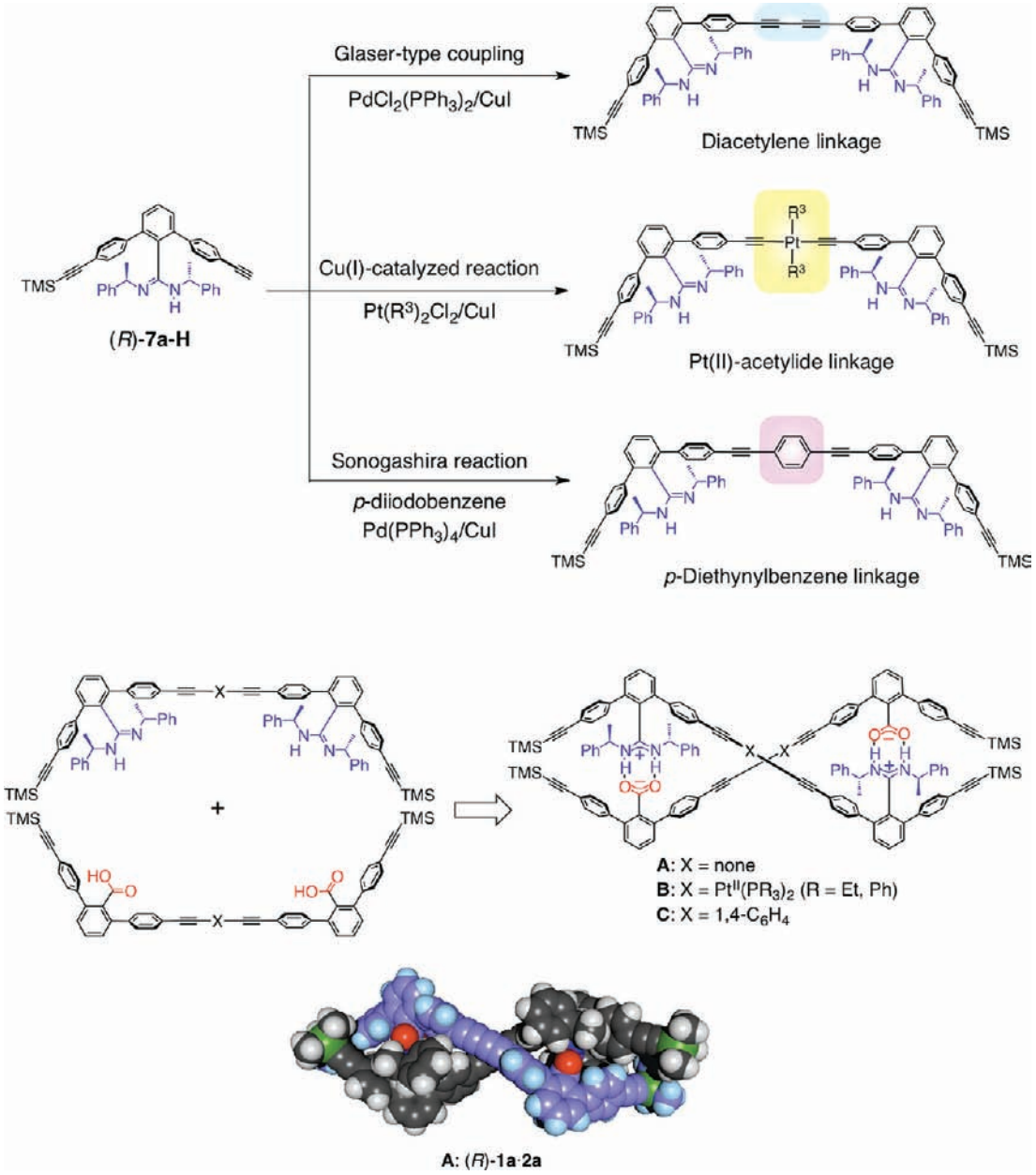

Figure 1. Modular strategy to construct a series of amidine dimers joined by various linkers (top), intertwined complementary double helix formation between chiral amidine and achiral carboxylic acid dimers (middle), and the crystal structure of the diacetylene-linked double helix (**A**: (*R*)-**1a**·**2a**) (bottom).

Recently, we developed a modular strategy to construct a series of rationally designed complementary double helices bound through amidinium−carboxylate salt bridges[16] that have a high stability and well-defined directionality (Figure 1).[17] The double helical structure relies on the crescent-shaped *m*-terphenyl-based, rigid π-conjugated backbones joined by diacetylene linkages, which prevent the duplex formation from taking any conformations other than the double helices. In addition, the helix-sense is readily controlled by the chirality introduced on the amidine groups. Duplex **A** composed of an achiral carboxylic acid dimer and an optically active (*R*)-1-phenylethyl amidine-bound dimer was found to adopt a right-handed double-helical structure as evidenced by an X-ray crystallographic analysis (A in Figure 1).[16a]

By taking advantage of this complementary amidine/carboxylic acid system, we have synthesized a series of complementary double helical oligomers[16b,e,k] and polymers[16c,h] linked by the *trans*-Pt(II) acetylide[16b,c,e,k,18] residues and *p*-diethynylbenzene units[16h] as the linker moieties based on the modular strategy that allows the one-step construction of amidine dimers and carboxylic acid dimers joined by the different linkers starting from the identical amidine ((*R*)-**7a**-**H**) and carboxylic acid monomers (**8a**-**H**, Scheme 1) by the Glaser-type coupling, Cu(I)-catalyzed reaction, and Sonogashira reaction, respectively (Figure 1), and the resulting complementary double helices (**B** and **C** in Figure 1, respectively, for dimers) also possess a helix-sense bias induced by the chiral amidine groups.

In the present study, we synthesized a series of chiral and achiral amidine and achiral carboxylic acid dimeric strands bearing three kinds of linker units, i.e., diacetylene, *trans*-Pt(II)-acetylide, and *p*-diethynylbenzene linkages, by the modular

dx.doi.org/10.1021/ja303701d | *J. Am. Chem. Soc.* 2012, 134, 9506−9520

Scheme 1. Synthesis of Diacetylene-Linked Amidine and Carboxylic Acid Dimers

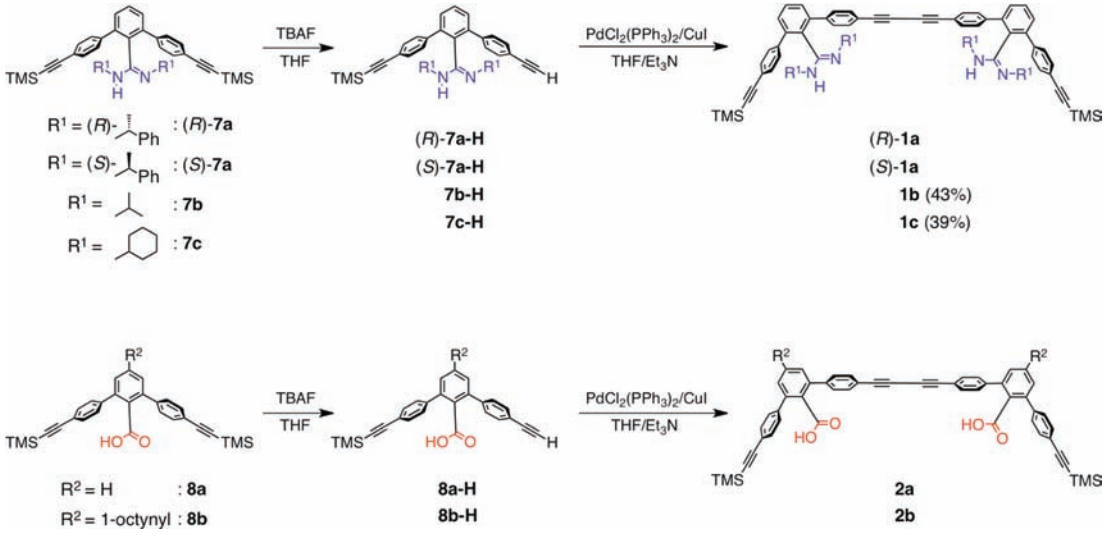

strategy (Chart 1), and investigated the effects of the linkages and the substituents on the amidine residues and those at the phenyl groups of the *p*-diethynylbenzene linkers on their complementary double helix formations by measuring the absorption, circular dichroism (CD), and ^{1}H NMR spectroscopies. The thermodynamic and kinetic stabilities of the complementary double helices stabilized by the amidinium–carboxylate salt bridges were also investigated in detail by determining the association constants for the double helix formation, the rates for the chain exchanges of the chiral double helices, and the helix-inversion barriers for racemic double helices composed of achiral amidines. The present results will not only contribute to a basic understanding of the principles underlying the formation of synthetic and biological double helices, but also provide a clue to developing rationally designed novel double helices with specific structures and functions. Although single-stranded helical foldamers, such as oligo(*m*-phenylene ethynylene)s, have been comprehensively investigated,[4c] there has been no report on the thermodynamics and kinetics of the double helix formation except for the seminal example of aromatic oligoamide-based double helices.[6t,8]

RESULTS AND DISCUSSION

Synthesis. The chiral/achiral amidine and carboxylic acid dimers joined by a variety of linkers (**A**, **B**, and **C** in Figure 1)[16a,b,h,k] were synthesized in a stepwise manner based on the modular approach by the Glaser-type coupling (Scheme 1), the Cu(I)-catalyzed reaction (Scheme 2), and the Sonogashira reaction (Scheme 3), respectively, starting from the monoethynyl amidine monomers ((*R*)- and (*S*)-**7a-H**, **7b-H**, and **7c-H**) and carboxylic acid monomers (**8a-H** and **8b-H**) with *m*-terphenyl groups as versatile building blocks, which had been prepared by the monodesilylation of the corresponding amidine monomers ((*R*)- and (*S*)-**7a**, **7b**, and **7c**) and carboxylic acid monomers (**8a** and **8b**) using tetra-*n*-butylammonium fluoride (TBAF) according to previously reported methods (Scheme 1).[16a,e,h,l] The monoethynyl carboxylic acid monomer bearing a 1-octynyl chain at the 5′-position of the *m*-terphenyl group (**8b**), which was introduced as a solubility enhancer for their oligomers and polymers,[16g,h,j,k] was also employed in this study.

Novel achiral amidine dimers (**1b** and **1c**) joined by diacetylene linkers were synthesized by the palladium-catalyzed Glaser-type homocoupling of the corresponding monoethynyl amidine monomers (**7b-H** and **7c-H**) in 43 and 39% yield, respectively (Scheme 1) according to the methods reported for the synthesis of the analogous chiral amidine dimers ((*R*)- and (*S*)-**1a**)[16a] and achiral carboxylic acid dimers (**2a** and **2b**).[16a,g]

The four chiral amidine dimers ((*R*)- and (*S*)-**3a** and -**3b**) and two achiral carboxylic acid dimers (**4a** and **4b**) bearing Pt(II)-acetylide linkers with triethylphosphine (PEt_3) or triphenylphosphine (PPh_3) ligands were synthesized by the Cu(I)-catalyzed reaction of the corresponding monoethynyl amidine monomers ((*R*)- and (*S*)-**7a-H**) and carboxylic acid monomer (**8a-H**) with $PtCl_2(PEt_3)_2$ or $PtCl_2(PPh_3)_2$, respectively, in the presence of diethylamine according to our previously reported methods (Scheme 2).[16b,k] In the same way, a novel achiral cyclohexyl-bound amidine Pt(II)-acetylide-linked dimer with PEt_3 ligands (**3c**) was prepared from **7c-H**[16l] in moderate yield (62%).

The novel chiral ((*S*)-**5a** and (*R*)-**5b** and -**5c**) and achiral amidine dimers (**5d**) and achiral carboxylic acid dimers (**6a**–**6e**) linked through *p*-diethynylbenzene units with electron-donating (2,5-dimethoxy) and/or electron-withdrawing (2,3,5,6-tetrafluoro, 2-nitro, or 2,5-dinitro) substituents at the phenyl groups were prepared from the corresponding monoethynyl amidine monomers ((*R*)- and (*S*)-**7a-H** and **7c-H**) and carboxylic acid monomer (**8a-H**) with *p*-diiodobenzene derivatives (**9a**–**9e**), respectively, by the palladium-catalyzed Sonogashira reaction in similar to the synthesis of (*R*)-**5a** and **6f**,[16h] giving the desired dimers in moderate yields (Scheme 3).

All the monomers and dimers were purified by column chromatography and characterized and identified by ^{1}H and ^{13}C or ^{31}P NMR spectroscopies, elemental analyses, and/or mass measurements (see the Supporting Information [SI]).

Complementary Double-Helix Formation. The chiral and achiral amidine dimers used in this study readily formed double helices with their complementary carboxylic acid dimers by mixing in a 1:1 molar ratio through salt bridge formations, as confirmed by the ^{1}H NMR and electron-spray ionization mass (ESI-MS) spectroscopies. Figure 2 shows the typical ^{1}H NMR spectra of the duplexes linked by diacetylene ((*R*)-**1a**·**2a**) (a),[16a] Pt(II)-acetylide with PEt_3 ligands ((*R*)-**3a**·**4a**) (b),[16k]

dx.doi.org/10.1021/ja303701d | J. Am. Chem. Soc. 2012, 134, 9506–9520

Chart 1. Structures of Chiral and Achiral Amidine and Achiral Carboxylic Acid Dimers Linked by a Variety of Linkers (A–C) and Amidine and Carboxylic Acid Monomers (D)

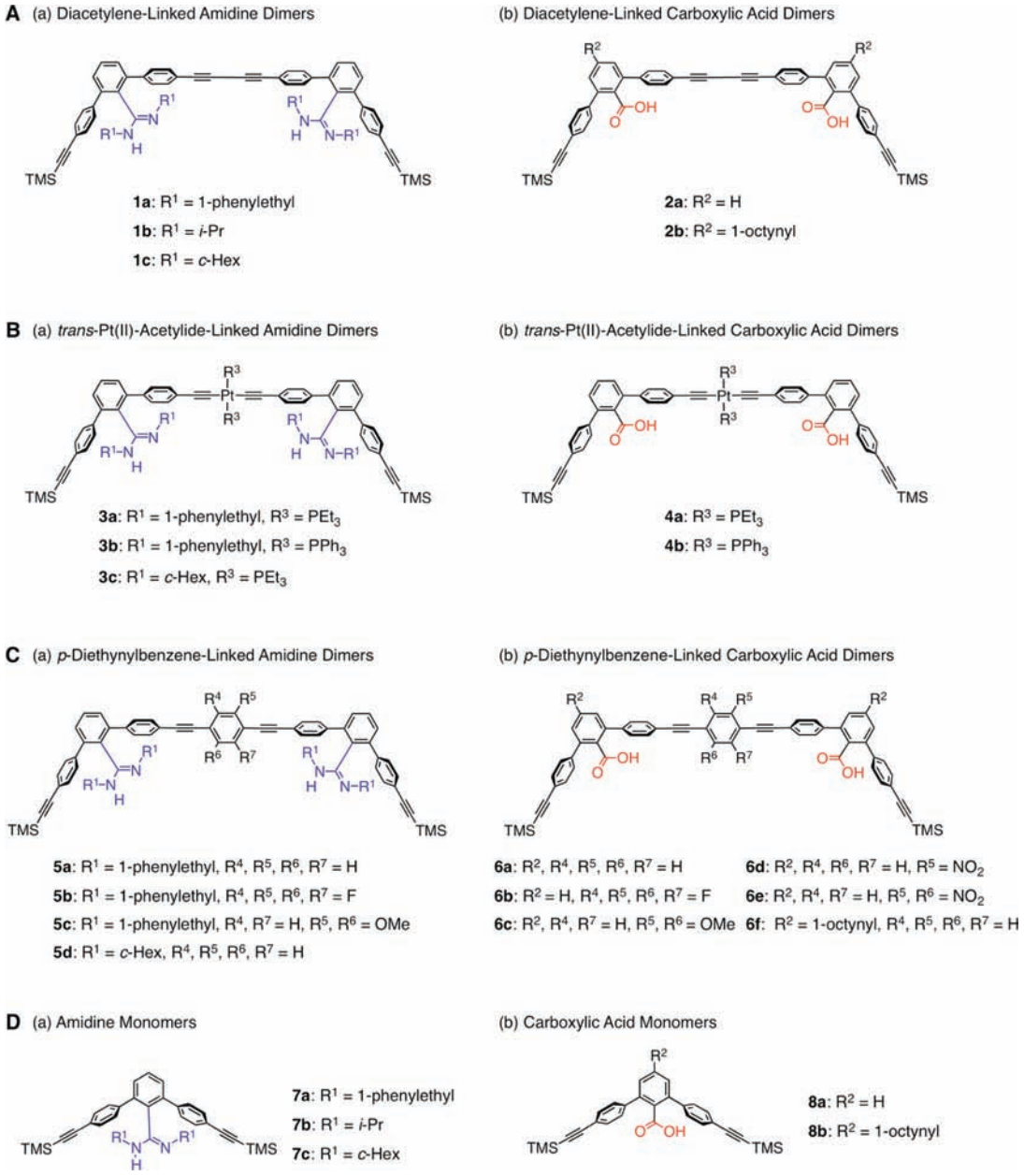

and *p*-diethynylbenzene ((*R*)-**5a**•**6a**) (c) linkages and a chiral amidine dimer strand ((*R*)-**5a**) (d) measured in $CDCl_3$ at 25 °C. As previously reported,[16a,k] the ^{1}H NMR spectra of the amidine dimer strands were complicated because of the *E*–*Z* isomerization of the C═N double bonds of the amidine residues,[16a,b,d,e,g–i,k] whereas the duplexes showed sets of clear signals including the salt-bridged N–H protons (c′ and c″) that appeared as two sharp doublets in the low magnetic fields (13–14 ppm) except for (*R*)-**3a**•**4a** (Figure 2 and Table S1 [SI]), and the methine (a′ and b′) and/or methyl protons (d′ and e′) of the amidine groups also gave two sets of signals; the nonequivalency of these signals support the double helical structures of the duplexes, since the monomer duplexes showed a one-doublet signal for the NH-protons (Table S1 [SI]). In contrast, the N–H protons in the duplex (*R*)-**3a**•**4a** (Figure 2b)[16k] as well as (*R*)-**3b**•**4b** (Table S1 [SI])[16b] were observed as two broadened doublets and singlet-like signals, respectively, indicating the salt-bridge formation as well as the molecular motion of the duplex that is slightly restricted probably due to the steric repulsion of the bulky phosphine ligands. Other racemic and optically active duplexes showed a similar tendency with clear salt-bridged N–H protons in the low magnetic fields (12–14 ppm) (Table S1 [SI]).

Figure 3A displays the typical CD spectra of the enantiomeric double helices with different linkers, but the same chiral amidine residues, (*R*)- and (*S*)-**1a**•**2a**,[16a] -**3a**•**4a**,[16k] and -**5a**•**6a** in $CHCl_3$ at 25 °C, which showed intense mirror image CD signals below ~370 nm, although their absorption and CD spectral patterns were different from each other, reflecting the difference in their linker structures, whereas the corresponding (*R*)- and (*S*)-amidine dimer strands (**1a**, **3a**, and **5a**) exhibited very weak CDs in the same regions (Figure S1,

dx.doi.org/10.1021/ja303701d | J. Am. Chem. Soc. 2012, 134, 9506–9520

Scheme 2. Synthesis of *trans*-Pt(II)-Acetylide-Linked Amidine and Carboxylic Acid Dimers

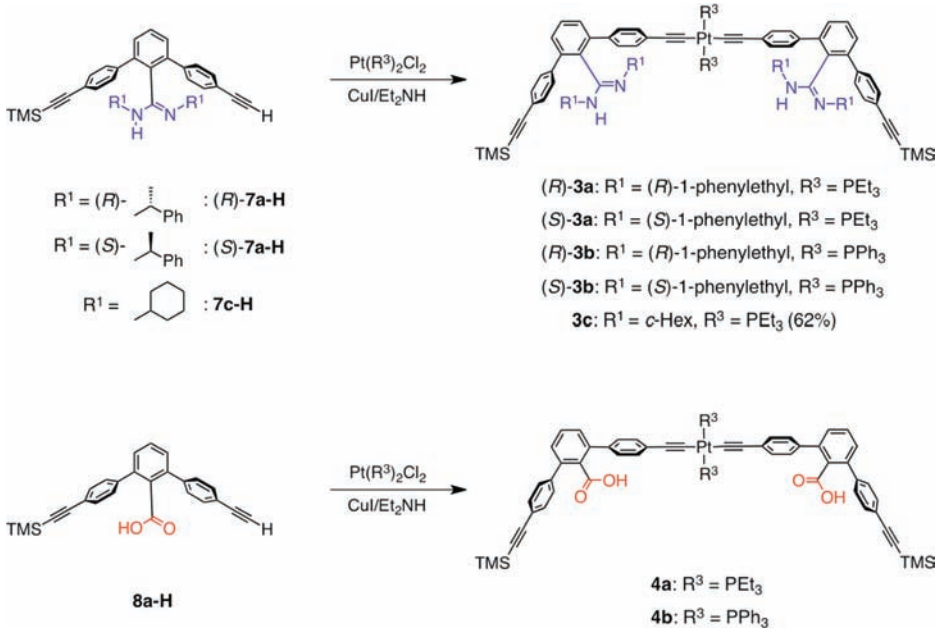

Scheme 3. Synthesis of *p*-Diethynylbenzene-Linked Amidine and Carboxylic Acid Dimers

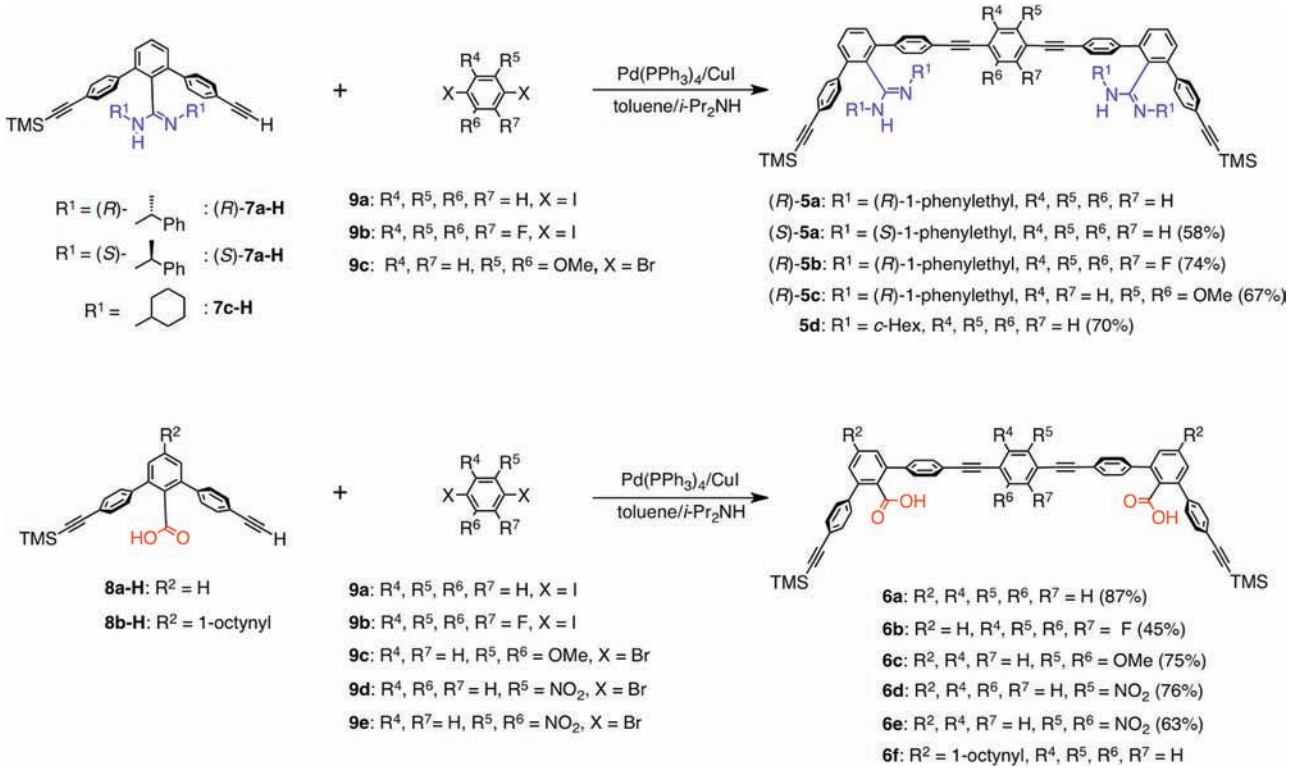

SI).[16a,k] The significant enhancements of the Cotton effect intensities were observed in the linker chromophore regions of the diacetylene (~300−370 nm) for **1a·2a**, the *trans*-Pt(II)-acetylide (~300−380 nm) for **3a·4a**, and the *p*-diethynylbenzene (~300−370 nm) for **5a·6a**, suggesting that **1a·2a**, **3a·4a**, and **5a·6a** appear to adopt an excess single-handed double helical structure. The Cotton effect signs of these duplexes with the same configuration at the amidine residues were roughly comparable to each other, suggesting that these dimers most probably take a double-helical structure with the same handedness when complexed with their complementary strands, i.e., the (*R*)-phenylethyl groups on the amidine residues may bias and induce the same right-handed double helices independent of the linker structures as evidenced by the X-ray crystallographic analysis result of the (*R*)-**1a·2a** (Figures 1 and S2A [SI]).[16a] Various attempts to obtain crystals of double-helical dimers of **3a·4a** and **5a·6a** suitable for an X-ray analysis produced only amorphous solids. Therefore, the energy minimized structures of the duplexes of (*R*)-**3a·4a** and (*R*)-**5a·6a** were constructed using the molecular mechanics (MM)

dx.doi.org/10.1021/ja303701d | J. Am. Chem. Soc. 2012, 134, 9506−9520

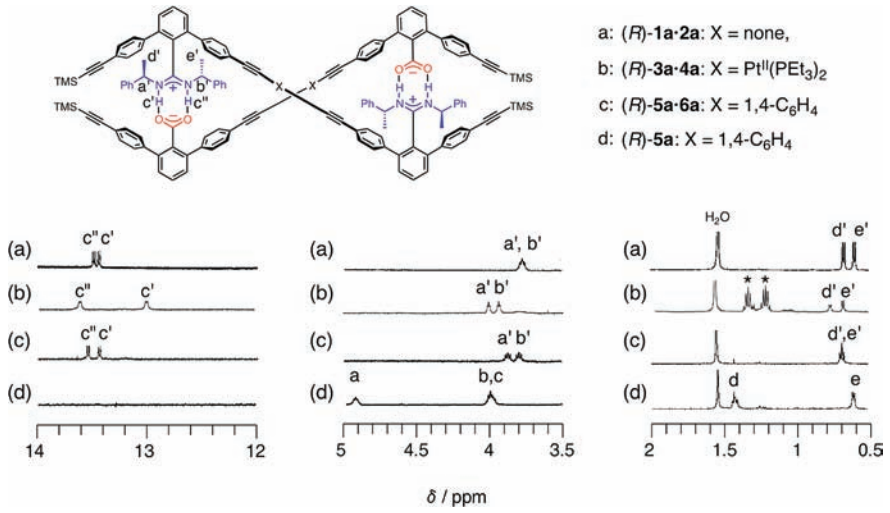

Figure 2. Partial ^{1}H NMR (500 MHz, 0.1 mM) spectra of (a) (*R*)-**1a·2a**, (b) (*R*)-**3a·4a**, (c) (*R*)-**5a·6a**, and (d) (*R*)-**5a** in $CDCl_3$ at 25 °C. The asterisks denote the signals derived from PEt_3 ligands.

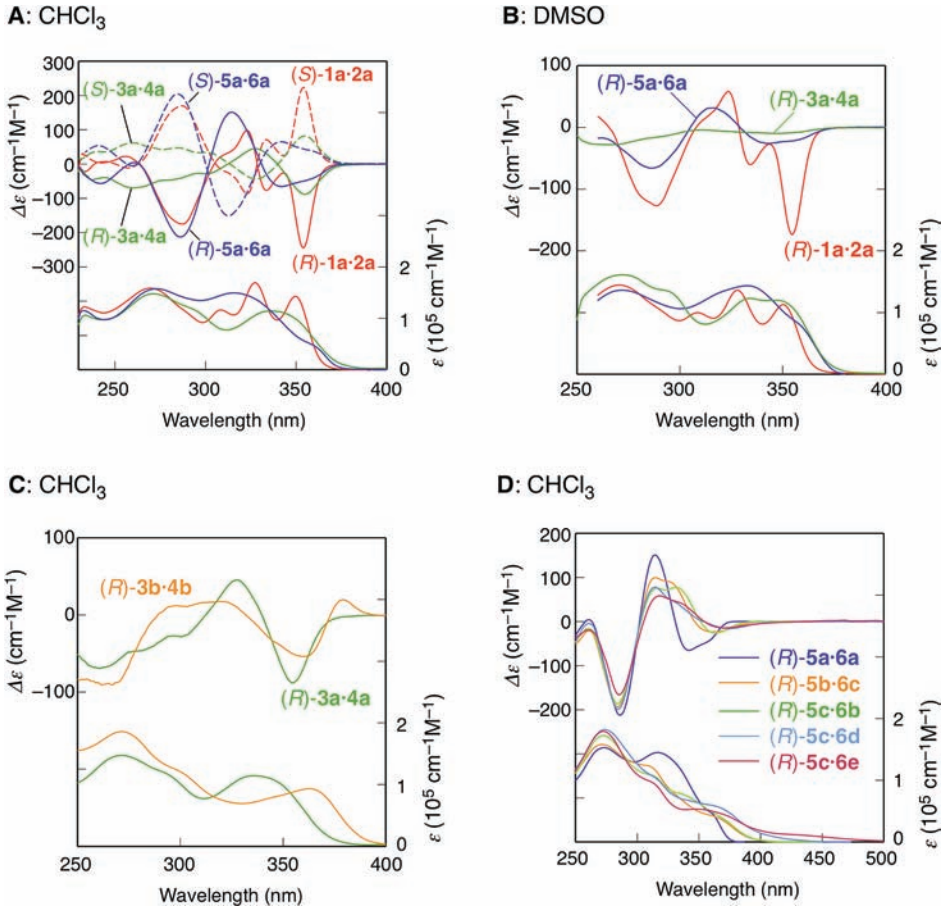

Figure 3. CD and absorption spectra (solid lines) of (*R*)-**1a·2a**, (*R*)-**3a·4a**, and (*R*)-**5a·6a** (0.1 mM) in $CHCl_3$ (A) and DMSO (B) at 25 °C. CD spectra (dashed lines) of (*S*)-**1a·2a**, (*S*)-**3a·4a**, and (*S*)-**5a·6a** (0.1 mM) in $CHCl_3$ are also shown in A. (C) CD and absorption spectra of (*R*)-**3a·4a** and (*R*)-**3b·4b** (0.1 mM) in $CHCl_3$ at 25 °C. (D) CD and absorption spectra of (*R*)-**5a·6a**, (*R*)-**5b·6c**, (*R*)-**5c·6b**, (*R*)-**5c·6d**, and (*R*)-**5c·6e** (0.1 mM) in $CHCl_3$ at 25 °C.

calculations based on analogous crystal structures.[16a,b,e,h] The calculated structure of (*R*)-**3a·4a** revealed a right-handed double-stranded helical structure (Figure S2B [SI]), in which the two Pt atoms at the linker moieties were located at a slightly long distance of 6.1 Å, due to the steric repulsion of the bulky phosphine ligands as in the case for an analogous dimeric double helix with the PPh_3 ligands (7.7 Å).[16b] In contrast, the calculated structure of (*R*)-**5a·6a** (Figure S2C [SI]) has the two aromatic rings of the *p*-diethynylbenzene moieties overlapping to each other with a distance of about 3.5 Å that is close to that between the diacetylene linkers of each strand observed in the X-ray structure of (*R*)-**1a·2a** (3.8 Å, Figures 1 and S2A [SI]).

dx.doi.org/10.1021/ja303701d | *J. Am. Chem. Soc.* 2012, 134, 9506−9520

Table 1. Association Constants of Duplexes at 25 °C

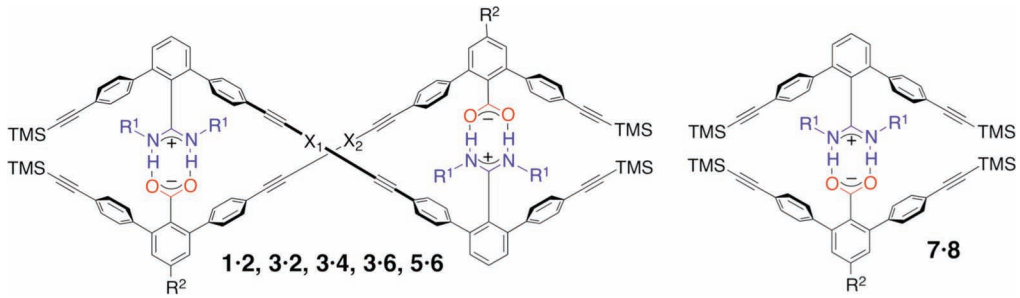

					$\Delta\varepsilon$ (cm^{-1} M^{-1})/λ (nm)		K_a(M^{-1})		
duplex	R^1	R^2	X^1	X^2	1st	2nd	$CHCl_3$[a]	THF[a]	DMSO[b]
7a·8a	(*R*)-1-phenylethyl	H	–	–	−169/289	39/264	2.82×10^6		~0
	(*S*)-1-phenylethyl	H	–	–	167/289	−41/264			
7a·8b	(*R*)-1-phenylethyl	1-octynyl	–	–	−166/290	36/265	3.47×10^6		
7b·8a	*i*-Pr	H	–	–	–	–	1.34×10^{6c}		
7c·8a	*c*-Hex	H	–	–	–	–	1.26×10^{7c}		
1a·2a	(*R*)-1-phenylethyl	H	none	none	−230/354	−76/334	6.43×10^{13}	1.87×10^6	3.8×10^4
	(*S*)-1-phenylethyl	H	none	none	223/354	71/334			
1b·2a	*i*-Pr	H	none	none	–	–	2.66×10^{12c}		
1c·2a	*c*-Hex	H	none	none	–	–	3.17×10^{14c}		
3b·2a	(*R*)-1-phenylethyl	H	$Pt(PPh_3)_2$	none	−78/353	−45/336	4.14×10^{11}		
3b·2b	(*R*)-1-phenylethyl	1-octynyl	$Pt(PPh_3)_2$	none	−79/353	−39/336	9.05×10^{11}		
3a·4a	(*R*)-1-phenylethyl	H	$Pt(PEt_3)_2$	$Pt(PEt_3)_2$	−88/355	45/328	5.10×10^{8d}		~0
	(S)-1-phenylethyl	H	$Pt(PEt_3)_2$	$Pt(PEt_3)_2$	82/355	−44/328			
3b·4b	(*R*)-1-phenylethyl	H	$Pt(PPh_3)_2$	$Pt(PPh_3)_2$	20/379	−54/360	1.08×10^7		~0
	(*S*)-1-phenylethyl	H	$Pt(PPh_3)_2$	$Pt(PPh_3)_2$	−20/379	54/360			
3b·6a	(*R*)-1-phenylethyl	H	$Pt(PPh_3)_2$	1,4-C_6H_4	−70/362	70/325	5.23×10^{11}		
3b·6b	(*R*)-1-phenylethyl	H	$Pt(PPh_3)_2$	1,4-C_6F_4	−49/359	54/328	4.97×10^{11}		
3b·6e	(*R*)-1-phenylethyl	H	$Pt(PPh_3)_2$	2,5-$(NO_2)_2$-1,4-C_6H_2	−20/358	21/329	3.21×10^{11}		
5a·6a	(*R*)-1-phenylethyl	H	1,4-C_6H_4	1,4-C_6H_4	−65/342	151/314	2.99×10^{12}	1.65×10^5	6.5×10^3
	(S)-1-phenylethyl	H	1,4-C_6H_4	1,4-C_6H_4	65/342	−151/314			
5a·6f	(*R*)-1-phenylethyl	1-octynyl	1,4-C_6H_4	1,4-C_6H_4	−69/342	136/314		2.2×10^{5e}	
5b·6c	(*R*)-1-phenylethyl	H	1,4-C_6F_4	2,5-$(MeO)_2$-1,4-C_6H_2	−23/362	99/315			2.4×10^4
5c·6b	(*R*)-1-phenylethyl	H	2,5-$(MeO)_2$-1,4-C_6H_2	1,4-C_6F_4	−26/364	78/331	1.12×10^{13}		6.6×10^4
5c·6d	(*R*)-1-phenylethyl	H	2,5-$(MeO)_2$-1,4-C_6H_2	2-NO_2-1,4-C_6H_3	−16/376	78/314			1.5×10^4
5c·6e	(*R*)-1-phenylethyl	H	$(MeO)_2$-1,4-C_6H_2	2,5-$(NO_2)_2$-1,4-C_6H_2	−15/370	58/318	4.82×10^{12}		2.9×10^4

[a]Estimated by CD titration. [b]Estimated by ^{1}H NMR. [c]Estimated by CD titration in the presence of an optically active duplex. [d]Cited from ref 16k. [e]Cited from ref 16h.

dx.doi.org/10.1021/ja303701d | J. Am. Chem. Soc. 2012, 134, 9506−9520

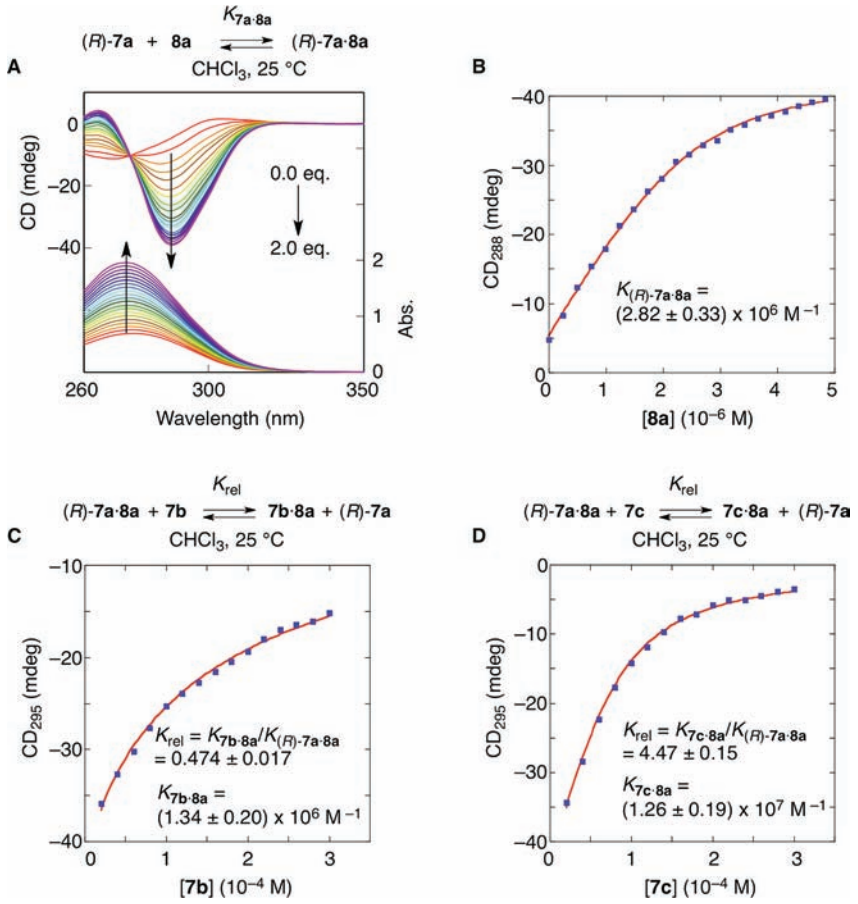

Figure 4. (A) CD and absorption spectral changes of (*R*)-**7a** ($c = 2.48 \times 10^{-6}$ M) upon the addition of **8a** in $CHCl_3$ at 25 °C. (B) Plots of the CD intensity at 288 nm vs [**8a**]. The curve in the plots was obtained by the curve-fitting method, giving the association constant of (*R*)-**7a·8a** ($K_{(R)\text{-}7a\cdot 8a}$) to be $(2.82 \pm 0.33) \times 10^6$ M^{-1}. (C) Plots of the CD intensity at 295 nm of (*R*)-**7a·8a** ($c = 1.00 \times 10^{-6}$ M) upon the addition of **7b** in $CHCl_3$ at 25 °C vs [**7b**]. (D) Plots of the CD intensity at 295 nm of (*R*)-**7a·8a** ($c = 1.00 \times 10^{-6}$ M) upon the addition of **7c** in $CHCl_3$ at 25 °C vs [**7c**]. The curves in C and D represent the curve-fittings according to the eq 4 in the SI. The relative association constants (K_{rel}) of **7b·8a** to (*R*)-**7a·8a** and **7c·8a** to (*R*)-**7a·8a** were then estimated to be 0.474 ± 0.017 and 4.47 ± 0.15, respectively, resulting in the $K_{7b\cdot 8a}$ and $K_{7c\cdot 8a}$ values to be $(1.34 \pm 0.20) \times 10^6$ and $(1.26 \pm 0.19) \times 10^7$ M^{-1}, respectively.

It should be noted that (*R*)-**1a·2a** and (*R*)-**5a·6a** exhibited intense Cotton effects even in DMSO in which the salt bridge formation is hampered, although the intensities were reduced to 67% and 28% of those in $CHCl_3$, respectively, whereas (*R*)-**3a·4a** showed a very weak CD similar to that of the amidine strand (*R*)-**3a**, indicating that the (*R*)-**3a·4a** duplex underwent dissociation into the (*R*)-**3a** and **4a** single strands in DMSO (Figure 3B). These remarkable solvent effects on the CD spectra closely relate to their stabilities of the duplexes in solution, being ascribed to the differences in their association constants depending on the linker structures (see below).

The Cotton effect signs and pattern of (*R*)-**3b·4b** with the more bulky PPh_3 ligands in the Pt(II)-acetylide linker chromophore region were almost similar to those of (*R*)-**3a·4a**, indicating that the bulkiness of the phosphine ligands hardly influences the helical sense, although the CD intensities of (*R*)-**3b·4b** were slightly weaker than those of (*R*)-**3a·4a**, and the absorption maximum shifted to a longer wavelength by ~27 nm in the absorption spectrum (Figure 3C).

The introduction of either electron-donating or electron-withdrawing substituents at the *p*-phenylene linkers of the duplexes ((*R*)-**5b·6c**, (*R*)-**5c·6b**, (*R*)-**5c·6d**, and (*R*)-**5c·6e**) gave rise to a considerable red-shift in their absorption spectra, and their CD spectral patterns in the linker chromophore regions also changed, while maintaining their Cotton effect signs when compared to those of the nonsubstituted duplex ((*R*)-**5a·6a**) (Figure 3D), indicating a charge-transfer complexation between the *p*-phenylene residues that may enhance the stability of their double helix formations with the same helix sense bias (see also Figure 6 and the text below).

Thermodynamic Stabilities of Monomeric and Dimeric Duplexes: Effect of Linkers. The effects of the linker moieties and the substituents on the amidine residues and those of the phenyl groups of the *p*-diethynylbenzene linkers on the stabilities of the complementary double helices were then investigated in terms of the association constants (K_a) by CD titrations combined with competition CD titrations. These results are summarized in Table 1.

First, the association constant of the monomeric duplex (*R*)-**7a·8a** was estimated by the direct CD titration of the amidine monomer (*R*)-**7a** with the carboxylic acid monomer **8a** in a similar way previously reported (Figure 4A).[16h] The CD intensity at the first Cotton effect increased with the increasing concentration of **8a** accompanied by a synchronous increase in its absorption intensity. The K_a for (*R*)-**7a·8a** was then calculated to be $(2.82 \pm 0.33) \times 10^6$ M^{-1} in $CHCl_3$ at 25 °C from the nonlinear least-squares curve fitting of the CD intensity (CD_{288}) at 288 nm (Figure 4B). The introduction of a

dx.doi.org/10.1021/ja303701d | J. Am. Chem. Soc. 2012, 134, 9506−9520

1-octynyl chain on the carboxylic acid unit did not significantly affect the association constant; the K_a for (*R*)-**7a**·**8b** was (3.47 ± 0.50) × 10^6 M^{-1} (Figure S3 [SI]). In the same way, the K_a values of the Pt(II)-acetylide-linked duplexes bearing PPh_3 ligands ((*R*)-**3b**·**4b**) and PEt_3 ligands ((*R*)-**3a**·**4a**)[16k] in $CHCl_3$ at 25 °C were estimated to be (1.08 ± 0.14) × 10^7 (Figure S4, SI) and (5.1 ± 2.2) × 10^8 M^{-1}, respectively, by the direct CD titration experiments.

In order to investigate the effects of the substituents on the amidine residues on the duplex formation of the monomers, the competition CD titration experiments were employed to estimate the K_a value ((1.34 ± 0.20) × 10^6 M^{-1}) between the isopropyl amidine-bound monomer **7b** and the carboxylic acid monomer **8a** in the presence of (*R*)-**7a**, while the K_a value of (*R*)-**7a**·**8a** was known as described above (Figures 4C and S5 and also the SI). In a similar fashion, the K_a value between the cyclohexyl amidine-bound **7c** and the carboxylic acid monomer **8a** was estimated to be (1.26 ± 0.19) × 10^7 M^{-1} (Figures 4D and S6 [SI]), which is 4.5 times greater than that of (*R*)-**7a**·**8a**.

The competition CD titration experiments were also employed to estimate the K_a values for the duplexes linked through the diacetylene and *p*-diethynylbenzene units, such as **1a**·**2a** and **5a**·**6a**, respectively, because their association constants were too high to be determined by the direct CD titration experiments even at concentrations as low as 10^{-7} M (i.e., the detection limit for our spectrophotometer using a 10-cm quartz cell.) Therefore, the K_a value for the duplex formation between (*R*)-**3b** and **2b** was first estimated as the base value by the competition CD titration experiments using the achiral carboxylic acid monomer **8b** (Figure 5A). The linker

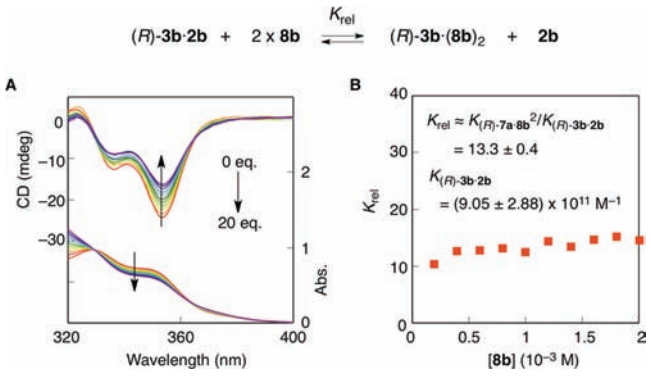

Figure 5. (A) CD and absorption spectral changes of duplex (*R*)-**3b**·**2b** (c = 1.01 × 10^{-4} M) upon the addition of **8b** in $CHCl_3$ at 25 °C. (B) Plots of the K_{rel} (based on the CD intensities at 353 nm) vs [**8b**]. For more detailed calculation procedures, see eqs 5−8 in the SI.

structures of (*R*)-**3b** and **2b**, in particular, their lengths were considerably different from each other, resulting in the formation of a heteroduplex with a smaller K_a suitable for the measurements. The CD intensity of the (*R*)-**3b**·**2b** duplex decreased with the increasing concentration of **8b**, resulting in the formation of the ternary complex (*R*)-**3b**·$(\mathbf{8b})_2$. Based on the changes in the CD intensities, the relative K_a value (K_{rel}) of (*R*)-**3b**·$(\mathbf{8b})_2$ to (*R*)-**3b**·**2b** can be approximately given by $K_{(R)\text{-}\mathbf{7a}\cdot\mathbf{8b}}{}^2/K_{(R)\text{-}\mathbf{3b}\cdot\mathbf{2b}}$ (13.3 ± 0.4), leading to the $K_{(R)\text{-}\mathbf{3b}\cdot\mathbf{2b}}$ value of (9.05 ± 2.88) × 10^{11} M^{-1} at 25 °C (Figure 5B) (for more detailed procedures, see the SI). Similarly, the K_a value of the duplex (*R*)-**3b**·**2a** in $CHCl_3$ was calculated to be (4.14 ± 1.29) × 10^{11} M^{-1} at 25 °C (Figure S7, SI). The competition CD titration experiments were further performed to estimate the K_a value of **1b**·**2a** in $CHCl_3$ at 25 °C ((2.66 ± 0.93) × 10^{12} M^{-1}) using the $K_{(R)\text{-}\mathbf{3b}\cdot\mathbf{2a}}$ as the base value (Figure S8 and the SI). The K_a values for the other duplexes in $CHCl_3$ at 25 °C were also estimated in a similar fashion by the competition CD titrations (Figures S9−S16, SI) and the results are summarized in Table 1.

On the basis of the association constant measurement results, the effects of the linker structures on the stabilities of the double helix formations were clearly revealed; the K_a values of (*R*)-**1a**·**2a** (6.43 × 10^{13} M^{-1}), (*R*)-**3a**·**4a** (5.10 × 10^8 M^{-1}), and (*R*)-**5a**·**6a** (2.99 × 10^{12} M^{-1}) in $CHCl_3$ at 25 °C increased in the following order: Pt(II)-acetylide linker < *p*-diethynylbenzene linker < diacetylene linker, which is in agreement with the reverse order of the bulkiness at the linkers. This tendency was also supported by the facts that the K_a values of the heteroduplexes formed between the Pt(II)-acetylide linked amidine dimer with PPh_3 ligands ((*R*)-**3b**) and the diacetylene-linked (**2a**) or *p*-diethynylbenzene-linked (**6a**) carboxylic acid dimer significantly decreased as compared to those of the corresponding homoduplexes, **1a**·**2a** and **5a**·**6a**, respectively (Table 1). A further comparison of the K_a values between (*R*)-**3a**·**4a** with PEt_3 ligands (5.10 × 10^8 M^{-1}) and (*R*)-**3b**·**4b** with PPh_3 ligands (1.08 × 10^7 M^{-1}) indicated that the bulkiness of the phosphine ligands at the Pt(II)-acetylide linkers destabilizes the double helical structure due to the steric repulsion caused by the more bulky PPh_3 ligands, as anticipated from their MM-calculated structures (Figure S2B, SI).[16b]

Effect of Substituents on Amidine Residues. By comparison of the observed K_a values for the duplexes between the carboxylic acid (**8a**) and amidine monomers (**7a**−**7c**) and the diacetylene-linked carboxylic acid (**2a**) and amidine dimers (**1a**−**1c**), the effect of the substituents on the amidine residues (isopropyl (*i*-Pr), (*R*)-1-phenylethyl, and cyclohexyl (*c*-Hex) groups) on the stabilities of the duplex formations were clearly revealed; the K_a values increased in the following order: *i*-Pr < (*R*)-1-phenylethyl < *c*-Hex for both of the monomers and dimers (Table 1). This order may not be consistent with the bulkiness nor basicity of the substituents on the amidine residues.[19] Although the reason is not presently clear, an interesting trend was observed when the K_a values of the monomeric and dimeric duplexes were compared in terms of $K_{2mer}/(K_{1mer})^2$, in which the K_{2mer} and K_{1mer} are the association constants for the dimers and monomers bearing the same substituents on the amidine residues, respectively; the $K_{2mer}/(K_{1mer})^2$ values were 1.48 for *c*-Hex, 2.00 for *i*-Pr, and 8.09 for (*R*)-1-phenylethyl. In all cases, the K_{2mer} values were higher than those of the $(K_{1mer})^2$ ones because of the synergistic effects. However, a noticeable synergistic gain was observed in the duplex bearing the chiral (*R*)-1-phenylethyl substituents on the amidine residues compared to those with the other achiral substituents. This remarkable synergy effect observed in the (*R*)-**1a**·**2a** duplex may arise from the strong helical sense bias of the chiral amidine substituents that are able to offer no choice other than to form a right-handed double helical conformation,[16a] while the achiral amidine substituents of **1b**·**2a** and **1c**·**2a** most likely produce interconvertible right- and left-handed helical conformations as supported by their variable-temperature ^{1}H NMR measurement results (see below). These differences in the possible helical conformations may more or less affect the thermodynamic stabilities of the duplexes.

Effect of Substituents on Phenylene Linkers. The introduction of either electron-donating (2,5-dimethoxy) or electron-withdrawing (2,3,5,6-tetrafluoro, 2-nitro or 2,5-dini-

tro) substituents at the *p*-phenylene linkers of the duplexes ((*R*)-**5b·6c**, (*R*)-**5c·6b**, (*R*)-**5c·6d**, and (*R*)-**5c·6e**) was found to stabilize the complementary double helix formations due to the charge-transfer interaction between the *p*-phenylene residues as compared to the nonsubstituted duplex ((*R*)-**5a·6a**); the K_a values increased from 2.99×10^{12} M^{-1} ((*R*)-**5a·6a**) to 1.12×10^{13} M^{-1} ((*R*)-**5c·6b**) and 4.82×10^{12} M^{-1} ((*R*)-**5c·6e**) in $CHCl_3$ at 25 °C (Table 1). Such charge-transfer interactions between the 2,5-dimethoxybenzene-linked amidine dimer ((*R*)-**5c**) and 2,5-dinitrobenzene-linked carboxylic acid dimer (**6e**) were supported by a visible color change in the (*R*)-**5c·6e** solution upon mixing the colorless solution of (*R*)-**5c** and the orange-yellow solution of **6e** in $CHCl_3$ (Figure 6C), and this color change was accompanied by a change in their absorption spectra, suggesting a charge-transfer complexation (Figure 6B).

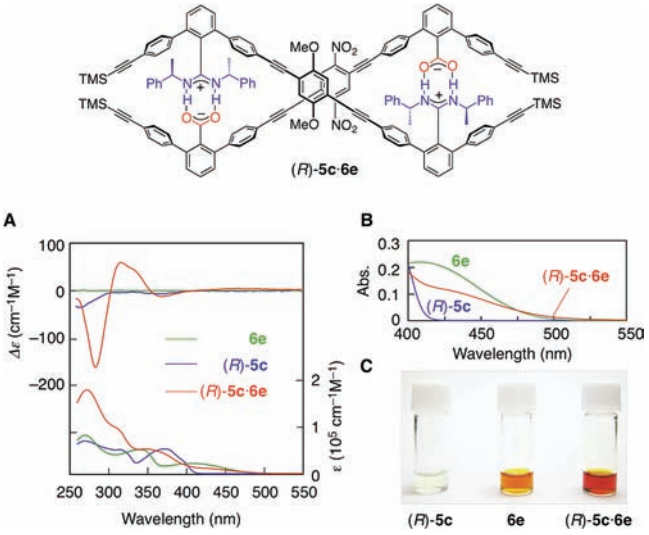

Figure 6. (A) CD and absorption spectra (0.1 mM) of (*R*)-**5c**, **6e**, and (*R*)-**5c·6e** in $CDCl_3$ at 25 °C. (B) Partial absorption spectra (0.1 mM) of (*R*)-**5c**, **6e**, and (*R*)-**5c·6e** in $CDCl_3$ at 25 °C. (C) Photographs of the solutions of (*R*)-**5c**, **6e**, and (*R*)-**5c·6e** in $CDCl_3$ at 25 °C.

As described above, the double helical conformations of the complementary duplexes are destabilized in DMSO because the salt bridge formations are hampered in DMSO. In fact, the CD intensity of the (*R*)-**5a·6a** duplex in DMSO was reduced to 28% of that in $CHCl_3$ (see Figure 3A,B). We then further investigated the effect of the substituents introduced at the *p*-phenylene linkers on the stabilities of the duplex formations in DMSO by estimating their K_a values along with measuring their CDs in DMSO. The K_a values of a series of substituted *p*-phenylene-linked duplexes were directly estimated from their ^{1}H NMR spectra. As a typical example, Figure 7A shows the ^{1}H NMR spectra of the TMS proton resonance region of a 1:1 mixture of (*R*)-**5c** and **6b** in DMSO-d_6 at 25 °C, showing four peaks being assignable to the single (*R*)-**5c** and **6b** strands and their duplex. Based on the integral ratio, the K_a value was estimated to be 6.6×10^4 M^{-1} at 25 °C. In the same manner, the K_a values of the other duplexes including the diacetylene-linked duplex ((*R*)-**1a·2a**) and the Pt(II)-acetylide linked duplex ((*R*)-**3a·4a**) in DMSO-d_6 were also estimated (Table 1). The obtained K_a values in DMSO-d_6 at 25 °C were found to increase in the order: (*R*)-**3a·4a** (~0 M^{-1}) < (*R*)-**5a·6a** (6.5×10^3 M^{-1}) < (*R*)-**1a·2a** (3.8×10^4 M^{-1}) as anticipated from that in $CHCl_3$.

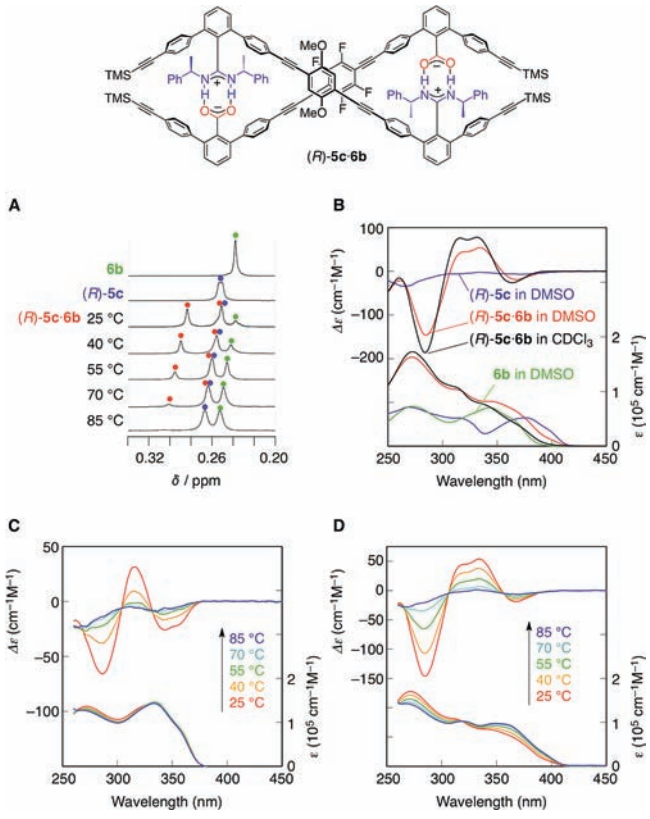

Figure 7. (A) Partial ^{1}H NMR (500 MHz, DMSO-d_6, 0.10 mM) spectra of **6b** and (*R*)-**5c** at 25 °C and the duplex (*R*)-**5c·6b** at various temperatures. The peaks of **6b**, (*R*)-**5c**, and (*R*)-**5c·6b** were denoted by green-, blue-, and red-filled circles, respectively. (B) CD and absorption spectra (0.1 mM) of (*R*)-**5c** and (*R*)-**5c·6b** and absorption spectrum (0.1 mM) of **6b** in DMSO at 25 °C. CD and absorption spectra (0.1 mM) of (*R*)-**5c·6b** in $CDCl_3$ at 25 °C are also shown. Temperature-dependent CD and absorption spectral changes (0.1 mM) of (*R*)-**5a·6a** (C) and (*R*)-**5c·6b** (D) in DMSO.

As observed in $CHCl_3$, the attractive charge-transfer interactions between the aromatic linkers bearing either electron-donating or electron-withdrawing substituents also enhanced the stabilities of the duplexes in DMSO-d_6, and the K_a values were estimated to be 2.4×10^4 M^{-1} for (*R*)-**5b·6c**, 6.6×10^4 M^{-1} for (*R*)-**5c·6b**, 1.5×10^4 M^{-1} for (*R*)-**5c·6d**, and 2.9×10^4 M^{-1} for (*R*)-**5c·6e** (Table 1); these values were significantly higher than that of the nonsubstituted (*R*)-**5a·6a** (6.5×10^3 M^{-1}) and comparable to that of the diacetylene-linked dimer (*R*)-**1a·2a** (3.8×10^4 M^{-1}). More importantly, the K_a value of (*R*)-**5c·6b** was much higher than that of (*R*)-**5a·6a** by a factor of ~10 in DMSO-d_6, whereas in $CHCl_3$, it was ~3.7 times. The charge-transfer interaction might efficiently contribute to stabilizing the duplex formation in DMSO-d_6, in which the salt bridges are diminished, while the salt bridge formation is extremely strong in $CHCl_3$ and determines the overall stability of the duplexes in $CHCl_3$. It should be noted that (*R*)-**5c·6b** even exhibited intense Cotton effects in DMSO, although the intensities were reduced to 78% of those in $CHCl_3$ (Figure 7B), which is still higher than that of the diacetylene-linked (*R*)-**1a·2a** (67%).

The variable-temperature CD measurements in DMSO more clearly demonstrated the contribution of the charge-transfer interactions to the stabilities of the duplexes (Figure 7C,D). Upon heating, the CD intensities of (*R*)-**5a·6a** rapidly

dx.doi.org/10.1021/ja303701d | *J. Am. Chem. Soc.* 2012, 134, 9506−9520

decreased and reached a constant value at around 70 °C, whose spectral pattern was identical to that of the (*R*)-**5a**, indicating the dissociation of the duplex (*R*)-**5a·6a** into (*R*)-**5a** and **6a** strands at that temperature (Figure 7C). In contrast, those of (*R*)-**5c·6b** were gradually decreased with the increasing temperature accompanied by a significant increase in the absorbance in the longer wavelength regions (hyperchromic effect), suggesting the dissociation of the (*R*)-**5c·6b** at around 80−85 °C (Figure 7D); a similar tendency was observed in the variable-temperature ^{1}H NMR spectra of (*R*)-**5c·6b** in DMSO-d_6 (Figure 7A). Consequently, the charge-transfer interactions were found to effectively contribute to stabilizing complementary double helices linked through the *p*-diethynylbenzene units, especially in polar solvents such as DMSO.

Kinetic Studies of Chain Exchange Reactions of Chiral Duplex. With the aim of elucidating the mechanism of the chain exchange process between the (*R*)-**1a** strand in the (*R*)-**1a·2a** double helix and its enantiomeric (*S*)-**1a** strand in $CDCl_3$, the kinetics of the chain exchange reaction were investigated using CD spectroscopies. Upon mixing of the equimolar amounts of (*R*)-**1a·2a** and (*S*)-**1a** in $CDCl_3$,[20] the chain exchange slowly took place to form the corresponding racemic double helices. Figure 8A shows the changes in the CD intensities of the (*R*)-**1a·2a**/(*S*)-**1a** mixture at 354 nm (the first negative Cotton effect) in $CDCl_3$ at various temperatures from 25 to 45 °C vs time. The CD intensity of the mixture gradually decreased with time and reached an equilibrium within 15 h at 25 °C and no detectable CD change was observed for 1 h thereafter, resulting from a very slow chain exchange process. The chain exchange process was analyzed according to eq 12 in the SI, and the reaction rate (k) for the (*R*)-**1a·2a**/(*S*)-**1a** mixture was then calculated based on the nonlinear least-squares curve fitting of the CD changes to be $k = 0.48\ M^{-1}\ s^{-1}$ at 25 °C, which corresponds to the half-life time (τ) of 2 h at 25 °C. In the same way, the k values of the (*R*)-**1a·2a**/(*S*)-**1a** mixture at various temperatures were estimated, showing a gradual increase in the k values with the increasing temperature. The activation parameters ($\Delta H^{\ddagger}$ and $\Delta S^{\ddagger}$) of the chain exchange process were then estimated to be 50.8 kJ mol^{-1} and −80.6 J mol^{-1} K^{-1}, respectively, based on the Eyring plot of the data (Figure 8B and Table 2). The negative $\Delta S^{\ddagger}$ value for the intermolecular chain exchange as well as the high K_a value for the duplex **1a·2a** indicated that the chain exchange reaction most likely proceeds via a direct exchange pathway (Figure 9A) that involves ternary complexation of (*R*)-**1a·2a**·(*S*)-**1a**, followed by dissociation of the (*R*)-**1a** strand.

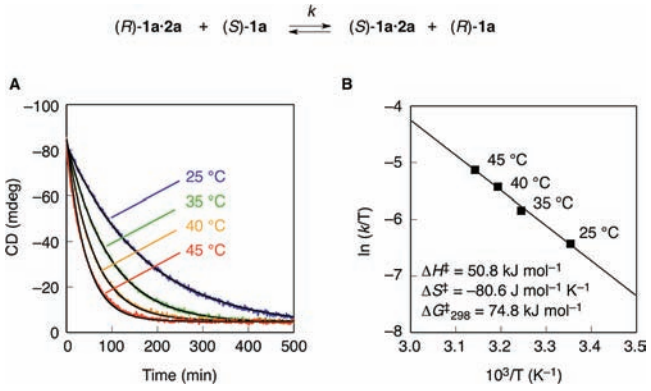

Figure 8. (A) Time-dependent CD intensity changes of (*R*)-**1a·2a** (0.1 mM) at 354 nm upon mixing an equimolar of (*S*)-**1a** in $CDCl_3$ at various temperatures (25−45 °C). (B) Eyring plot for the chain exchange rates estimated at 25 to 45 °C, where the thermodynamic parameters ($\Delta H^{\ddagger}$, $\Delta S^{\ddagger}$, and $\Delta G_{298}{}^{\ddagger}$) were estimated according to the following equation, $\ln k/T = -\Delta H^{\ddagger}/R\cdot(1/T) + \ln k_B/h + \Delta S^{\ddagger}/R$. The curves in A were obtained by the curve-fittings according to the eq 12 in the SI.

The k values and the activation parameters ($\Delta H^{\ddagger}$ and $\Delta S^{\ddagger}$) of the chain exchange processes for the Pt(II)-acetylide linked duplexes **3a·4a** and **3b·4b** and the *p*-diethynylbenzene linked duplex **5a·6a** were then estimated in a similar fashion (Figures S17−S19, SI) and the results are summarized in Table 2. As a consequence, the chain exchange rates (k) increased in the order: diacetylene linker < *p*-diethynylbenzene linker < Pt(II)$(PEt_3)_2$-acetylide linker < Pt(II)$(PPh_3)_2$-acetylide linker. Again, this order is in agreement with the order of the bulkiness. Judging from the smaller, but negative $\Delta S^{\ddagger}$ for the duplex **5a·6a**, the chain exchange appears to proceed via a direct exchange one as well as the duplex **1a·2a** (Figure 9A). In sharp contrast, the $\Delta S^{\ddagger}$ values for the Pt(II)-acetylide linked duplexes **3a·4a** and **3b·4b** were positive, 81.1 and 53.5 J mol^{-1} K^{-1}, respectively (Table 2), suggesting that the chain exchange reactions take place not via a direct exchange pathway, but via a dissociation−exchange one (Figure 9B).

Helix-Inversion Kinetics and Barriers of Double Helices. The temperature-dependent ^{1}H NMR measurements of four racemic dimer duplexes carrying achiral amidine residues (Table 3) in $CDCl_3$ or CD_2Cl_2 were performed in order to observe their helix-inversion processes and to estimate their helix-inversion barriers under slow exchange conditions. In contrast to the optically active dimer duplexes, the diacetylene linked racemic duplex **1c·2b** showed a rather sharp doublet due to the N−H proton resonances for the salt bridges at 12.22 ppm at 25 °C (Figure 10B), whereas the salt-bridged N−H protons (c′ and c″) of the optically active dimer duplexes appeared as two sets of nonequivalent doublets ("outer" and "inner" N−H protons, respectively) (see Figure 2a−c) that originated from the stable preferred-handed double helical structures. These results suggest that the rate of helix inversion of the racemic duplex **1c·2b** was too fast at 25 °C for the present NMR time scale to distinguish the nonequivalent N−H protons due to the right- and left-handed double helical states of the duplex via rotation along the C−C bond between the amidine and *m*-terphenyl groups as shown in Figure 10A (bottom).

Upon cooling to a low temperature, the salt-bridged N−H proton resonances of **1c·2b** became broadened and coalesced at −26 °C (Figure S20, SI). The N−H signal finally appeared as two sets of nonequivalent signals (12.279 and 12.156 ppm) at −60 °C as observed for (*R*)-**1a·2a**. The coalescence temperature (T_c = −26 °C) along with the chemical shift difference between the signals at −60 °C ($\Delta\nu$ = 61.5 Hz) made it possible to estimate the free energy of activation ($\Delta G^{\ddagger}$) for the helix-inversion of the duplex **1c·2b** to be 50.0 kJ mol^{-1} at 25 °C, which corresponds to the lifetime of the one-handed helical state (τ) of 9.37×10^{-5} s at 25 °C. The T_c, $\Delta G^{\ddagger}$, and τ values for the helix-inversion of the other racemic double helices **1b·2a**, **3c·4a**, and **5d·6a** were also attempted to be estimated in a similar fashion (Figures S21−S23, SI) and the results are summarized in Table 3. The salt-bridged N−H proton resonances of the diacetylene-linked **1b·2a** carrying isopropyl groups on the amidine residues also split into two sets of signals at low temperatures with a coalescence temperature of −47 °C (Figure S21, SI), giving a slightly lower $\Delta G^{\ddagger}$ value than that of

dx.doi.org/10.1021/ja303701d | J. Am. Chem. Soc. 2012, 134, 9506−9520

Table 2. Rates of Chain Exchange Reactions in $CDCl_3$

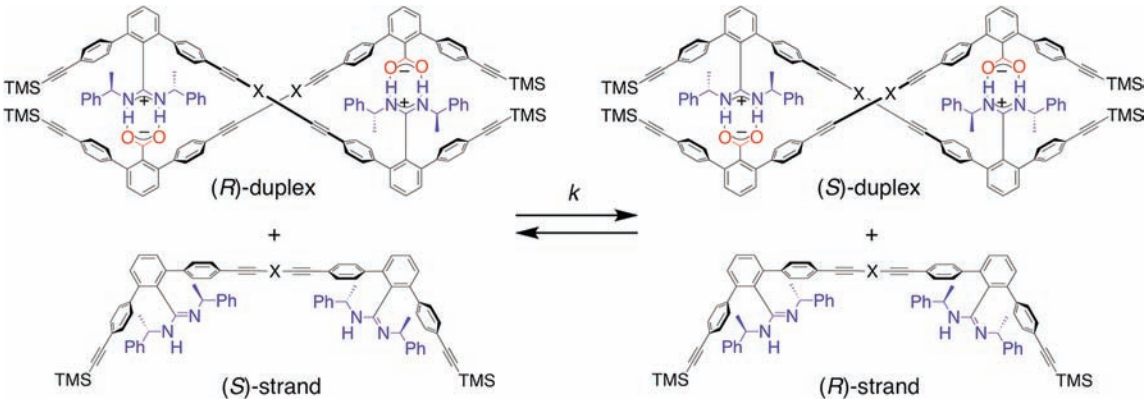

duplex	X	$k(M^{-1}\ s^{-1})$ at 25 °C	$t_{1/2}$ at 25 °C	$\Delta G^{\ddagger}_{298}$(kJ/mol)	$\Delta H^{\ddagger}$ (kJ/mol)	$\Delta S^{\ddagger}$ (J/mol·K)
1a·2a	none	0.48	2 h	74.8	50.8	−80.6
3a·4a	*trans*-Pt$(PEt_3)_2$	57	61 s	63.1	87.2	81.1
3b·4b	*trans*-Pt$(PPh_3)_2$	379	9 s	58.2	74.2	53.5
5a·6a	1,4-C_6H_4	6.4	9.1 min	68.4	58.7	−32.5

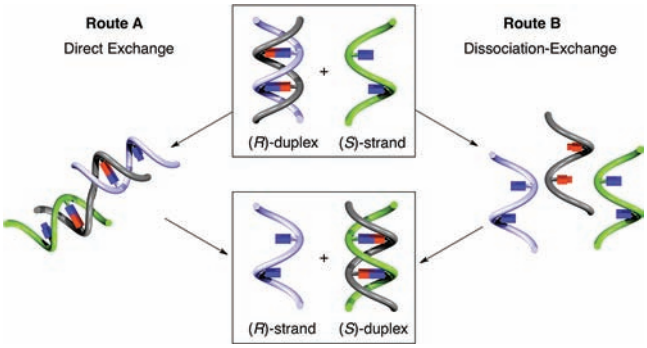

Figure 9. Schematic illustration of possible mechanisms (routes A and B) of the chain exchange between the (*R*)-duplex and (*S*)-strand.

the **1c·2b** duplex. These results indicate that the substituents on the amidine groups do not significantly affect the helix-inversion barrier for the diacetylene-linked dimers.

In contrast, the Pt(II)-acetylide linked duplex **3c·4a** and the *p*-diethynylbenzene linked duplex **5d·6a** did not show such a coalescence temperature due to helix-inversion even at −80 °C. The N−H protons of the Pt(II)-acetylide linked duplex **3c·4a** appeared as one broad doublet at 25 °C, which gradually broadened upon cooling accompanied by a significant upfield shift, but a clear coalescence point due to helix-inversion could not be observed at −80 °C in CD_2Cl_2. This unexpected high upfield shift of the N−H protons of **3c·4a** that was not observed for the diacetylene-linked dimers (Figures S20 and S21, SI) and broadening of the NH proton resonances of **3c·4a** may be related to a slow chain exchange between each strand via a dissociation−exchange pathway (see Figure 9 and Table 2), and its coalescence temperature due to helix-inversion could be presumed to be lower than −80 °C. Similar broad NH proton resonances were also observed for the *p*-diethynylbenzene linked duplex **5d·6a** at temperatures from 25 to −80 °C, indicating that the helix-inversion rate of racemic dimers was significantly influenced by the linker structures and the barriers for the helix-inversion increased in the following order: Pt(II)-acetylide linker, *p*-diethynylbenzene linker < diacetylene linker.

■ CONCLUSIONS

In conclusion, we have successfully synthesized a series of optically active and achiral amidine dimers and their complementary achiral carboxylic acid dimers joined by different linkers, such as diacetylene, Pt(II)-acetylide, and *p*-diethynylbenzene linkages, using a modular strategy. We have

Table 3. Rates of Helix-Inversion

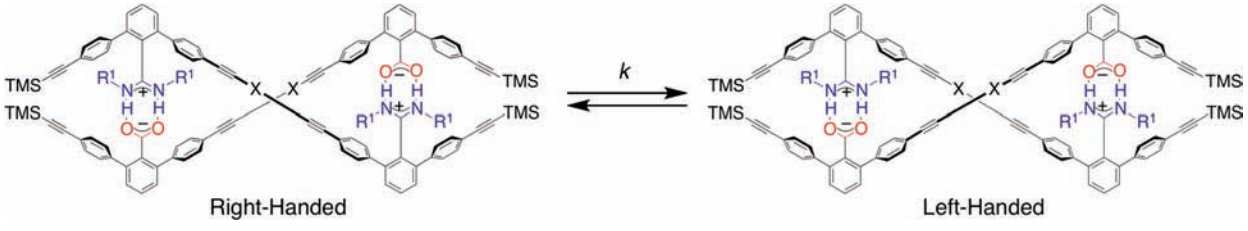

duplex	X	R^1	solvent	T_C (°C)[a]	$G^{\ddagger}_{298}$(kJ/mol)	τ_{298} (s)[b]
1b·2a	none	*i*-Pr	$CDC1_3$	−47	45.8	1.71×10^{-5}
1c·2b	none	*c*-Hex	$CDC1_3$	−26	50.0	9.37×10^{-5}
3c·4a	*trans*-Pt$(PEt_3)_2$	*c*-Hex	CD_2C1_2	<−80[c]	–	–
5d·6a	1,4-C_6H_4	*c*-Hex	CD_2C1_2	<−80[c]	–	–

[a]Coalescence temperature. [b]Life time of the one-handed helical state at 25 °C. [c]Coalescence temperature was not observed.

dx.doi.org/10.1021/ja303701d | *J. Am. Chem. Soc.* 2012, 134, 9506−9520

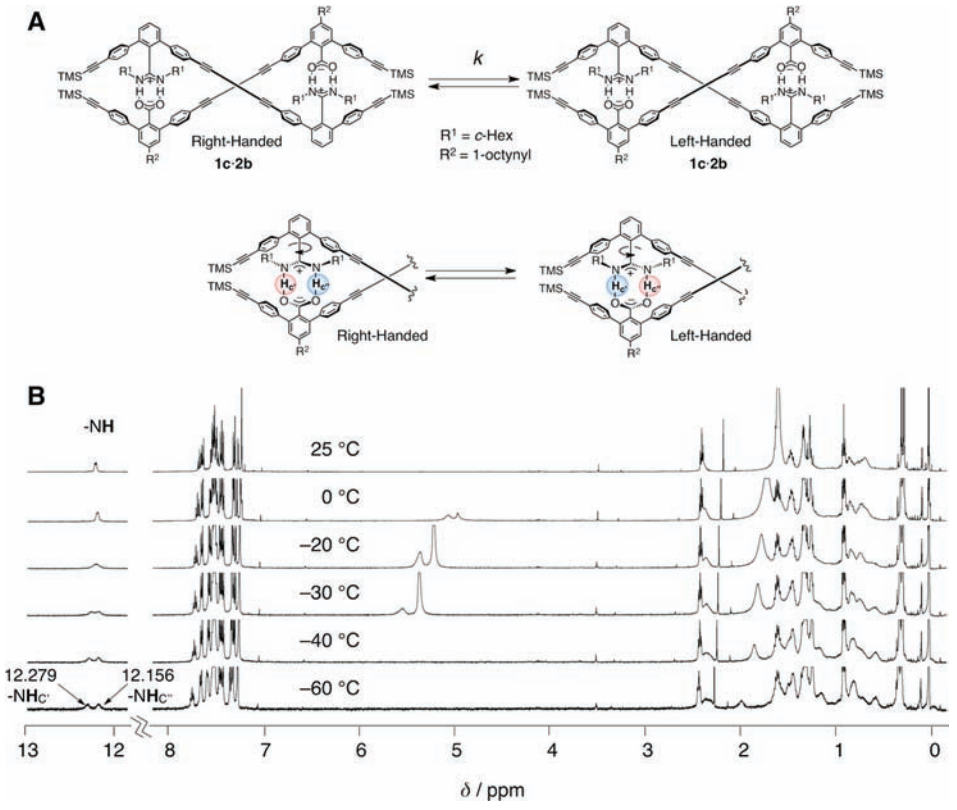

Figure 10. (A) Helix-inversion of duplex **1c·2b**. (B) Variable-temperature ^{1}H NMR spectra of **1c·2b** (500 MHz, $CDCl_3$, 2.0 mM) from −60 to 25 °C (those from −28 to −23 °C to estimate T_c, see Figure S20B, SI).

found that the thermodynamic and kinetic stabilities of the complementary double helix formations assisted by the amidinium−carboxylate salt bridges have a remarkable dependence on the linker structures, and are also affected by the substituents on the amidine groups. The thermodynamic analyses of the chiral dimer duplexes revealed that the association constants increase in the following order: Pt(II)-acetylide linker < *p*-diethynylbenzene linker < diacetylene linker, which is in agreement with the reverse order of the bulkiness. The substituents on the amidine groups were also found to affect the stabilities upon duplex formation, and the association constants of the duplexes increased in the following order: *i*-Pr < (*R*)-1-phenylethyl < *c*-Hex. During the formation of the *p*-diethynylbenzene-linked double helices, the charge-transfer interactions were found to contribute to stabilizing the double helices, especially in polar solvents such as DMSO, in which the salt bridge formation is significantly hampered. The kinetic analyses of the chain exchange reactions revealed a different mechanism that depends on the linker structures; i.e., the dissociation−exchange pathways are predominant for the Pt(II)-acetylide linked duplexes, while a direct chain exchange takes place for the diacetylene-linked and *p*-diethynylbenzene-linked duplexes. The present systematic studies on the mechanistic, thermodynamic, and kinetic stabilities of the complementary double helix formations assisted by amidinium−carboxylate salt bridges provide a clue not only for the development of novel double helices with specific functions, but also a possible strategy for template synthesis and an artificial replication system based on the complementary double helix formation.[16j] Studies along this line are currently ongoing in our laboratory.

■ ASSOCIATED CONTENT

Supporting Information

Full experimental details. This material is available free of charge via the Internet at http://pubs.acs.org.

■ AUTHOR INFORMATION

Corresponding Author

yashima@apchem.nagoya-u.ac.jp

Present Address

†Molecular Engineering Institute, Kinki University, Kayano-mori, Iizuka, Fukuoka 820-8555, Japan.

Notes

The authors declare no competing financial interest.

■ ACKNOWLEDGMENTS

This work was supported in part by Grants-in-Aid for Scientific Research (S) from the Japan Society for the Promotion of Science (JSPS) (E.Y.) and for Scientific Research on Innovative Areas, "Emergence in Chemistry" (20111010) from the MEXT (Y.F.). H.Y. expresses his thanks for a JSPS Research Fellowship for Young Scientists (No. 2728). We thank Drs. Takeshi Maeda and Kazuhiro Miwa for their help in the synthesis of the amidine and carboxylic acid dimers.

■ REFERENCES

(1) Pauling, L.; Corey, R. B.; Branson, H. R. *Proc. Natl. Acad. Sci. U.S.A.* **1951**, *37*, 205−211.
(2) Watson, J. D.; Crick, F. C. H. *Nature* **1953**, *171*, 737−738.
(3) (a) Schulz, G. E.; Schirmer, R. H. *Principles of Protein Structure*; Springer-Verlag: New York, 1979. (b) Saenger, W. *Principles of Nucleic Acid Structure*; Springer-Verlag: New York, 1984.

(4) (a) Okamoto, Y.; Nakano, T. *Chem. Rev.* **1994**, *94*, 349−372. (b) Rowan, A. E.; Nolte, R. J. M. *Angew. Chem., Int. Ed.* **1998**, *37*, 63−68. (c) Hill, D. J.; Mio, M. J.; Prince, R. B.; Hughes, T. S.; Moore, J. S. *Chem. Rev.* **2001**, *101*, 3893−4011.

(5) For reviews on synthetic helical polymers, see: (a) Green, M. M.; Peterson, N. C.; Sato, T.; Teramoto, A.; Cook, R.; Lifson, S. *Science* **1995**, *268*, 1860−1866. (b) Green, M. M.; Park, J.-W.; Sato, T.; Teramoto, A.; Lifson, S.; Selinger, R. L. B.; Selinger, J. V. *Angew. Chem., Int. Ed.* **1999**, *38*, 3138−3154. (c) Cornelissen, J. J. L. M.; Rowan, A. E.; Nolte, R. J. M.; Sommerdijk, N. A. J. M. *Chem. Rev.* **2001**, *101*, 4039−4070. (d) Fujiki, M. *Macromol. Rapid Commun.* **2001**, *22*, 539−563. (e) Nakano, T.; Okamoto, Y. *Chem. Rev.* **2001**, *101*, 4013−4038. (f) Yashima, E.; Maeda, K.; Nishimura, T. *Chem.—Eur. J.* **2004**, *10*, 42−51. (g) Lam, J. W. Y.; Tang, B. Z. *Acc. Chem. Res.* **2005**, *38*, 745−754. (h) Maeda, K.; Yashima, E. *Top. Curr. Chem.* **2006**, *265*, 47−88. (i) Masuda, T. *J. Polym. Sci., Part A: Polym. Chem.* **2007**, *45*, 165−180. (j) Kim, H.-J.; Lim, Y.-B.; Lee, M. *J. Polym. Sci., Part A: Polym. Chem.* **2008**, *46*, 1925−1935. (k) Pijper, D.; Feringa, B. L. *Soft Matter* **2008**, *4*, 1349−1372. (l) Rudick, J. G.; Percec, V. *Acc. Chem. Res.* **2008**, *41*, 1641−1652. (m) Yashima, E.; Maeda, K. *Macromolecules* **2008**, *41*, 3−12. (n) Yashima, E.; Maeda, K.; Furusho, Y. *Acc. Chem. Res.* **2008**, *41*, 1166−1180. (o) Kumaki, J.; Sakurai, S.-i.; Yashima, E. *Chem. Soc. Rev.* **2009**, *38*, 737−746. (p) Liu, J.; Lam, J. W. Y.; Tang, B. Z. *Chem. Rev.* **2009**, *109*, 5799−5867. (q) Yashima, E.; Maeda, K.; Iida, H.; Furusho, Y.; Nagai, K. *Chem. Rev.* **2009**, *109*, 6102−6211. (r) Fujiki, M. *Chem. Rec.* **2009**, *9*, 271−298. (s) Yashima, E. *Polym. J.* **2010**, *42*, 3−16. (t) Schwartz, E.; Koepf, M.; Kitto, H. J.; Nolte, R. J. M.; Rowan, A. E. *Polym. Chem.* **2011**, *2*, 33−47.

(6) For reviews on foldamers, see: (a) Gellman, S. H. *Acc. Chem. Res.* **1998**, *31*, 173−180. (b) Cheng, R. P.; Gellman, S. H.; DeGrado, W. F. *Chem. Rev.* **2001**, *101*, 3219−3232. (c) Brunsveld, L.; Folmer, B. J. B.; Meijer, E. W.; Sijbesma, R. P. *Chem. Rev.* **2001**, *101*, 4071−4097. (d) Huc, I. *Eur. J. Org. Chem.* **2004**, 17−29. (e) Seebach, D.; Beck, A. K.; Bierbaum, D. J. *Chem. Biodiversity* **2004**, *1*, 1111−1239. (f) Sanford, A. R.; Yamato, K.; Yang, X.; Yuan, L.; Han, Y.; Gong, B. *Eur. J. Biochem.* **2004**, *271*, 1416−1425. (g) Ray, C. R.; Moore, J. S. *Adv. Polym. Sci.* **2005**, *177*, 91−149. (h) Hoeben, F. J. M.; Jonkheijm, P.; Meijer, E. W.; Schenning, A. P. H. J. *Chem. Rev.* **2005**, *105*, 1491−1546. (i) Lockman, J. W.; Paul, N. M.; Parquette, J. R. *Prog. Polym. Sci.* **2005**, *30*, 423−452. (j) Stone, M. T.; Heemstra, J. M.; Moore, J. S. *Acc. Chem. Res.* **2006**, *39*, 11−20. (k) Li, Z.-T.; Hou, J.-L.; Li, C.; Yi, H.-P. *Chem. −Asian J.* **2006**, *1*, 766−778. (l) Hecht, S.; Huc, I. *Foldamers: Structure, Properties, and Applications*; Wiley−VCH: Weinheim, Germany, 2007. (m) Inai, Y.; Komori, H.; Ousaka, N. *Chem. Rec.* **2007**, *7*, 191−202. (n) Horne, W. S.; Gellman, S. H. *Acc. Chem. Res.* **2008**, *41*, 1399−1408. (o) Saraogi, I.; Hamilton, A. D. *Chem. Soc. Rev.* **2009**, *38*, 1726−1743. (p) Ni, B.-B.; Yan, Q.; Ma, Y.; Zhao, D. *Coord. Chem. Rev.* **2010**, *254*, 954−971. (q) Juwarker, H.; Jeong, K.-S. *Chem. Soc. Rev.* **2010**, *39*, 3664−3674. (r) Zhao, X.; Li, Z.-T. *Chem. Commun.* **2010**, *46*, 1601−1616. (s) Vasudev, P. G.; Chatterjee, S.; Shamala, N.; Balaram, P. *Chem. Rev.* **2011**, *111*, 657−687. (t) Guichard, G.; Huc, I. *Chem. Commun.* **2011**, *47*, 5933−5941. (u) Roy, A.; Prabhakaran, P.; Baruah, P. K.; Sanjayan, G. J. *Chem. Commun.* **2011**, *47*, 11593−11611.

(7) For reviews on synthetic double helices, see: (a) Constable, E. C. *Tetrahedron* **1992**, *48*, 10013−10059. (b) Lehn, J.-M. *Supramolecular Chemistry: Concepts and Perspectives*; VCH: Weinheim, Germany, 1995. (c) Piguet, C.; Bernardinelli, G.; Hopfgartner, G. *Chem. Rev.* **1997**, *97*, 2005−2062. (d) Albrecht, M. *Chem. Rev.* **2001**, *101*, 3457−3497. (e) Furusho, Y.; Yashima, E. *J. Synth. Org. Chem., Jpn.* **2007**, *65*, 1121−1133. (f) Furusho, Y.; Yashima, E. *Chem. Rec.* **2007**, *7*, 1−11. (g) Amemiya, R.; Yamaguchi, M. *Org. Biomol. Chem.* **2008**, *6*, 26−35. (h) Furusho, Y.; Yashima, E. *J. Polym. Sci., Part A: Polym. Chem.* **2009**, *47*, 5195−5207. (i) Haldar, D.; Schmuck, C. *Chem. Soc. Rev.* **2009**, *38*, 363−371. (j) Furusho, Y.; Yashima, E. *Macromol. Rapid Commun.* **2011**, *32*, 136−146. (k) Howson, S. E.; Scott, P. *Dalton Trans.* **2011**, *40*, 10268−10277.

(8) For examples of aromatic oligoamides that fold into double helices, see: (a) Berl, V.; Huc, I.; Khoury, R. G.; Krische, M. J.; Lehn, J.-M. *Nature* **2000**, *407*, 720−723. (b) Berl, V.; Huc, I.; Khoury, R. G.; Lehn, J.-M. *Chem.—Eur. J.* **2001**, *7*, 2810−2820. (c) Dolain, C.; Zhan, C.; Leger, J.-M.; Daniels, L.; Huc, I. *J. Am. Chem. Soc.* **2005**, *127*, 2400−2401. (d) Haldar, D.; Jiang, H.; Leger, J.-M.; Huc, I. *Angew. Chem., Int. Ed.* **2006**, *45*, 5483−5486. (e) Zhan, C.; Leger, J.-M.; Huc, I. *Angew. Chem., Int. Ed.* **2006**, *45*, 4625−4628. (f) Berni, E.; Kauffmann, B.; Bao, C.; Lefeuvre, J.; Bassani, D. M.; Huc, I. *Chem. −Eur. J.* **2007**, *13*, 8463−8469. (g) Gan, Q.; Bao, C.; Kauffmann, B.; Grelard, A.; Xiang, J.; Liu, S.; Huc, I.; Jiang, H. *Angew. Chem., Int. Ed.* **2008**, *47*, 1715−1718. (h) Ferrand, Y.; Kendhale, A. M.; Garric, J.; Kauffmann, B.; Huc, I. *Angew. Chem., Int. Ed.* **2010**, *49*, 1778−1781. (i) Baptiste, B.; Zhu, J.; Haldar, D.; Kauffmann, B.; Leger, J.-M.; Huc, I. *Chem.—Asian J.* **2010**, *5*, 1364−1375. (j) Ferrand, Y.; Gan, Q.; Kauffmann, B.; Jiang, H.; Huc, I. *Angew. Chem., Int. Ed.* **2011**, *50*, 7572−7575.

(9) For poly- and oligo(*m*-phenylene)-based double helices, see: (a) Goto, H.; Katagiri, H.; Furusho, Y.; Yashima, E. *J. Am. Chem. Soc.* **2006**, *128*, 7176−7178. (b) Goto, H.; Furusho, Y.; Yashima, E. *J. Am. Chem. Soc.* **2007**, *129*, 9168−9174. (c) Goto, H.; Furusho, Y.; Yashima, E. *J. Am. Chem. Soc.* **2007**, *129*, 109−112. (d) Ben, T.; Goto, H.; Miwa, K.; Goto, H.; Morino, K.; Furusho, Y.; Yashima, E. *Macromolecules* **2008**, *41*, 4506−4509. (e) Ben, T.; Furusho, Y.; Goto, H.; Miwa, K.; Yashima, E. *Org. Biomol. Chem.* **2009**, *7*, 2509−2512. (f) Goto, H.; Furusho, Y.; Miwa, K.; Yashima, E. *J. Am. Chem. Soc.* **2009**, *131*, 4710−4719.

(10) For examples of ion-templated double helices, see: (a) Sánchez-Quesada, J.; Seel, C.; Prados, P.; de Mendoza, J.; Dalcol, I.; Giralt, E. *J. Am. Chem. Soc.* **1996**, *118*, 277−278. (b) Keegan, J.; Kruger, P. E.; Nieuwenhuyzen, M.; O'Brien, J.; Martin, N. *Chem. Commun.* **2001**, 2192−2193. (c) Coles, S. J.; Frey, J. G.; Gale, P. A.; Hursthouse, M. B.; Light, M. E.; Navakhun, K.; Thomas, G. L. *Chem. Commun.* **2003**, 568−569. (d) Sugimoto, T.; Suzuki, T.; Shinkai, S.; Sada, K. *J. Am. Chem. Soc.* **2007**, *129*, 270−271. (e) Kim, H.-J.; Lee, E.; Kim, M. G.; Kim, M.-C.; Lee, M.; Sim, E. *Chem.—Eur. J.* **2008**, *14*, 3883−3888. (f) Haketa, Y.; Maeda, H. *Chem.—Eur. J.* **2011**, *17*, 1485−1492. For template-directed double helical polymers, see: (g) Yang, H.-C.; Lin, S.-Y.; Yang, H.-C.; Lin, C.-L.; Tsai, L.; Huang, S.-L.; Chen, I. W.-P.; Chen, C.-h.; Jin, B.-Y.; Luh, T.-Y. *Angew. Chem., Int. Ed.* **2006**, *45*, 726−730. (h) Lin, N.-T.; Lin, S.-Y.; Lee, S.-L.; Chen, C.-h.; Hsu, C.-H.; Hwang, L. P.; Xie, Z.-Y.; Chen, C.-h.; Huang, S.-L.; Luh, T.-Y. *Angew. Chem., Int. Ed.* **2007**, *46*, 4481−4485. (i) Yang, H.-C.; Lee, S.-L.; Chen, C.-h.; Lin, N.-T.; Yang, H.-C.; Jin, B.-Y.; Luh, T.-Y. *Chem. Commun.* **2008**, 6158−6160.

(11) For helicene-based double helices, see: (a) Sugiura, H.; Nigorikawa, Y.; Saiki, Y.; Nakamura, K.; Yamaguchi, M. *J. Am. Chem. Soc.* **2004**, *126*, 14858−14864. (b) Sugiura, H.; Yamaguchi, M. *Chem. Lett.* **2007**, *36*, 58−59. (c) Sugiura, H.; Amemiya, R.; Yamaguchi, M. *Chem.—Asian J.* **2008**, *3*, 244−260. (d) Amemiya, R.; Saito, N.; Yamaguchi, M. *J. Org. Chem.* **2008**, *73*, 7137−7144. (e) Saito, N.; Terakawa, R.; Shigeno, M.; Amemiya, R.; Yamaguchi, M. *J. Org. Chem.* **2011**, *76*, 4841−4858.

(12) For reviews and leading examples of PNA, see: (a) Nielsen, P. E.; Egholm, M.; Berg, R. H.; Buchardt, O. *Science* **1991**, *254*, 1497−1500. (b) Wittung, P.; Nielsen, P. E.; Buchardt, O.; Egholm, M.; Norden, B. *Nature* **1994**, *368*, 561−563. (c) Wittung, P.; Eriksson, M.; Lyng, R.; Nielsen, P. E.; Norden, B. *J. Am. Chem. Soc.* **1995**, *117*, 10167−10173. (d) Nielsen, P. E. *Acc. Chem. Res.* **1999**, *32*, 624−630. (e) Sforza, S.; Haaima, G.; Marchelli, R.; Nielsen, P. E. *Eur. J. Org. Chem.* **1999**, 197−204. (f) Totsingan, F.; Jain, V.; Bracken, W. C.; Faccini, A.; Tedeschi, T.; Marchelli, R.; Corradini, R.; Kallenbach, N. R.; Green, M. M. *Macromolecules* **2010**, *43*, 2692−2703.

(13) For examples of helicates, see: (a) Carrano, C. J.; Raymond, K. N. *J. Am. Chem. Soc.* **1978**, *100*, 5371−5374. (b) Lehn, J.-M.; Rigault, A.; Siegel, J.; Harrowfield, J.; Chevrier, B.; Moras, D. *Proc. Natl. Acad. Sci. U.S.A.* **1987**, *84*, 2565−2569. (c) Koert, U.; Harding, M. M.; Lehn, J.-M. *Nature* **1990**, *346*, 339−342. (d) Zarges, W.; Hall, J.; Lehn, J.-M.; Bolm, C. *Helv. Chim. Acta* **1991**, *74*, 1843−1852. (e) Kramer, R.; Lehn, J.-M.; De Cian, A.; Fischer, J. *Angew. Chem., Int. Ed. Engl.* **1993**, *32*, 703−706. (f) Charbonniere, L. J.; Bernardinelli, G.; Piguet, C.; Sargeson, A. M.; Williams, A. F. *J. Chem. Soc., Chem. Commun.* **1994**,

1419−1420. (g) Hasenknopf, B.; Lehn, J.-M. *Helv. Chim. Acta* **1996**, *79*, 1643−1650. (h) Woods, C. R.; Benaglia, M.; Cozzi, F.; Siegel, J. S. *Angew. Chem., Int. Ed. Engl.* **1996**, *35*, 1830−1833. (i) Orita, A.; Nakano, T.; An, D. L.; Tanikawa, K.; Wakamatsu, K.; Otera, J. *J. Am. Chem. Soc.* **2004**, *126*, 10389−10396. (j) Katagiri, H.; Miyagawa, T.; Furusho, Y.; Yashima, E. *Angew. Chem., Int. Ed.* **2006**, *45*, 1741−1744. (k) Stomeo, F.; Lincheneau, C.; Leonard, J. P.; O'Brein, J. E.; Peacock, R. D.; McCoy, C. P.; Gunnlaugsson, T. *J. Am. Chem. Soc.* **2009**, *131*, 9636−9637. (l) Miwa, K.; Furusho, Y.; Yashima, E. *Nat. Chem.* **2010**, *2*, 444−449. (m) Furusho, Y.; Miwa, K.; Asai, R.; Yashima, E. *Chem. −Eur. J.* **2011**, *17*, 13954−13957. (n) Albrecht, M.; Isaak, E.; Baumert, M.; Gossen, V.; Raabe, G.; Fröhlich, R. *Angew. Chem., Int. Ed.* **2011**, *50*, 2850−2853. (o) Howson, S. E.; Bolhuis, A.; Brabec, V.; Clarkson, G. J.; Malina, J.; Rodger, A.; Scott, P. *Nat. Chem.* **2012**, *4*, 31−36.

(14) For examples of hydrogen bonding-driven duplexes, see: (a) Sessler, J. L.; Wang, R. *J. Am. Chem. Soc.* **1996**, *118*, 9808−9809. (b) Gong, B.; Yan, Y.; Zeng, H.; Skrzypczak-Jankunn, E.; Kim, Y. W.; Zhu, J.; Ickes, H. *J. Am. Chem. Soc.* **1999**, *121*, 5607−5608. (c) Folmer, B. J. B.; Sijbesma, R. P.; Kooijman, H.; Spek, A. L.; Meijer, E. W. *J. Am. Chem. Soc.* **1999**, *121*, 9001−9007. (d) Corbin, P. S.; Zimmerman, S. C. *J. Am. Chem. Soc.* **2000**, *122*, 3779−3780. (e) Archer, E. A.; Goldberg, N. T.; Lynch, V.; Krische, M. J. *J. Am. Chem. Soc.* **2000**, *122*, 5006−5007. (f) Nowick, J. S.; Chung, D. M.; Maitra, K.; Maitra, S.; Stigers, K. D.; Sun, Y. *J. Am. Chem. Soc.* **2000**, *122*, 7654−7661. (g) Bisson, A. P.; Carver, F. J.; Eggleston, D. S.; Haltiwanger, R. C.; Hunter, C. A.; Livingstone, D. L.; McCabe, J. F.; Rotger, C.; Rowan, A. E. *J. Am. Chem. Soc.* **2000**, *122*, 8856−8868. (h) Corbin, P. S.; Zimmerman, S. C.; Thiessen, P. A.; Hawryluk, N. A.; Murray, T. J. *J. Am. Chem. Soc.* **2001**, *123*, 10475−10488. (i) Zeng, H.; Yang, X.; Flowers, R. A.; Gong, B. *J. Am. Chem. Soc.* **2002**, *124*, 2903−2910. (j) Moriuchi, T.; Tamura, T.; Hirao, T. *J. Am. Chem. Soc.* **2002**, *124*, 9356−9357. (k) Gong, H.; Krische, M. J. *J. Am. Chem. Soc.* **2005**, *127*, 1719−1725. (l) Zhu, J.; Lin, J.-B.; Xu, Y.-X.; Shao, X.-B.; Jiang, X.-K.; Li, Z.-T. *J. Am. Chem. Soc.* **2006**, *128*, 12307−12313. (m) Djurdjevic, S.; Leigh, D. A.; McNab, H.; Parsons, S.; Teobaldi, G.; Zerbetto, F. *J. Am. Chem. Soc.* **2007**, *129*, 476−477. (n) Yang, Y.; Xiang, J.-F.; Xue, M.; Hu, H.-Y.; Chen, C.-F. *J. Org. Chem.* **2008**, *73*, 6369−6377. (o) Chu, W.-J.; Yang, Y.; Chen, C.-F. *Org. Lett.* **2010**, *12*, 3156−3159. (p) Zeng, J.; Wang, W.; Deng, P.; Feng, W.; Zhou, J.; Yang, Y.; Yuan, L.; Yamato, K.; Gong, B. *Org. Lett.* **2011**, *13*, 3798−3801.

(15) For examples of complementary double helices, see: (a) Hasenknopf, B.; Lehn, J.-M.; Baum, G.; Fenske, D. *Proc. Natl. Acad. Sci. U. S. A.* **1996**, *93*, 1397−1400. (b) Li, L.; Wisner, J. A.; Jennings, M. C. *Org. Lett.* **2007**, *9*, 3267−3269. (c) Gan, Q.; Li, F.; Li, G.; Kauffmann, B.; Xiang, J.; Huc, I.; Jiang, H. *Chem. Commun.* **2010**, *46*, 297−299. (d) Wang, H.-B.; Mudraboyina, B. P.; Li, J.; Wisner, J. A. *Chem. Commun.* **2010**, *46*, 7343−7345.

(16) For artificial double helices based on amidinium−carboxylate salt bridges, see: (a) Tanaka, Y.; Katagiri, H.; Furusho, Y.; Yashima, E. *Angew. Chem., Int. Ed.* **2005**, *44*, 3867−3870. (b) Furusho, Y.; Tanaka, Y.; Yashima, E. *Org. Lett.* **2006**, *8*, 2583−2586. (c) Ikeda, M.; Tanaka, Y.; Hasegawa, T.; Furusho, Y.; Yashima, E. *J. Am. Chem. Soc.* **2006**, *128*, 6806−6807. (d) Furusho, Y.; Tanaka, Y.; Maeda, T.; Ikeda, M.; Yashima, E. *Chem. Commun.* **2007**, 3174−3176. (e) Hasegawa, T.; Furusho, Y.; Katagiri, H.; Yashima, E. *Angew. Chem., Int. Ed.* **2007**, *46*, 5885−5888. (f) Katagiri, H.; Tanaka, Y.; Furusho, Y.; Yashima, E. *Angew. Chem., Int. Ed.* **2007**, *46*, 2435−2439. (g) Ito, H.; Furusho, Y.; Hasegawa, T.; Yashima, E. *J. Am. Chem. Soc.* **2008**, *130*, 14008−14015. (h) Maeda, T.; Furusho, Y.; Sakurai, S.-i.; Kumaki, J.; Okoshi, K.; Yashima, E. *J. Am. Chem. Soc.* **2008**, *130*, 7938−7945. (i) Iida, H.; Shimoyama, M.; Furusho, Y.; Yashima, E. *J. Org. Chem.* **2010**, *75*, 417−423. (j) Yamada, H.; Furusho, Y.; Ito, H.; Yashima, E. *Chem. Commun.* **2010**, *46*, 3487−3489. (k) Ito, H.; Ikeda, M.; Hasegawa, T.; Furusho, Y.; Yashima, E. *J. Am. Chem. Soc.* **2011**, *133*, 3419−3432. (l) Yamada, H.; Furusho, Y.; Yashima, E. *J. Am. Chem. Soc.* **2012**, *134*, 7250−7253.

(17) The amidinium−carboxylate salt bridges have been widely utilized as a versatile scaffold to construct a number of supramolecules involved capsules and also as a template for molecular imprinting and autocatalytic systems, due to its charge-assisted, double hydrogen bonding and the high tolerance toward various functional groups. For examples, see: (a) Terfort, A.; von Kiedrowski, G. *Angew. Chem., Int. Ed. Engl.* **1992**, *31*, 654−656. (b) Félix, O.; Hosseini, M. W.; De Cian, A.; Fischer, J. *Angew. Chem., Int. Ed. Engl.* **1997**, *36*, 102−104. (c) Wulff, G.; Schönfeld, R. *Adv. Mater.* **1998**, *10*, 957−959. (d) Kraft, A.; Peters, L.; Powell, H. R. *Tetrahedron* **2002**, *58*, 3499−3505. (e) Corbellini, F.; Di Costanzo, L.; Crego-Calama, M.; Geremia, S.; Reinhoudt, D. N. *J. Am. Chem. Soc.* **2003**, *125*, 9946−9947. (f) Otsuki, J.; Iwasaki, K.; Nakano, Y.; Itou, M.; Araki, Y.; Ito, O. *Chem.—Eur. J.* **2004**, *10*, 3461−3466. (g) Damrauer, N. H.; Hodgkiss, J. M.; Rosenthal, J.; Nocera, D. G. *J. Phys. Chem. B* **2004**, *108*, 6315−6321. (h) Cooke, G.; Duclairoir, F. M. A.; Kraft, A.; Rosair, C.; Rotello, V. M. *Tetrahedron Lett.* **2004**, *45*, 557−560. (i) Rosenthal, J.; Hodgkiss, J. M.; Young, E. R.; Nocera, D. G. *J. Am. Chem. Soc.* **2006**, *128*, 10474−10483. (j) Otsuki, J.; Kanazawa, Y.; Kaito, A.; Islam, D.-M. S.; Araki, Y.; Ito, O. *Chem. −Eur. J.* **2008**, *14*, 3776−3784.

(18) Metal acetylide complexes, such as the Pt(II)−acetylide, can be used as useful components to construct well-defined two- and three-dimensional supramolecular architectures owing to their synthetic accessibility of Pt(II)−acetylides as well as the kinetic inertness of the robust Pt(II)−alkynyl linkage, see: (a) Stang, P. J.; Olenyuk, B. *Acc. Chem. Res.* **1997**, *30*, 502−518. (b) Yam, V. W.-W. *Acc. Chem. Res.* **2002**, *35*, 555−563. (c) Onitsuka, K.; Takahashi, S. *Top. Curr. Chem.* **2003**, *228*, 39−63. (d) Szafert, S.; Gladysz, J. A. *Chem. Rev.* **2006**, *106*, PR1−PR33. (e) Leung, S. Y.-L.; Tam., A. Y.-Y.; Tao, C.-H.; Chow, H. S.; Yam, V. W.-W. *J. Am. Chem. Soc.* **2012**, *134*, 1047−1056.

(19) The reported pK_a values of the conjugated acids of analogous amidines (see below) in aqueous solutions obtained by calculations using Advance Chemistry Development (ACD/Laboratories) Software (v11.02, SciFinder database) are as follows, indicating the basicity increases in the order: 1-phenylethyl < *c*-Hex < *i*-Pr, which is not consistent with that of the K_a values of the monomers and dimers.

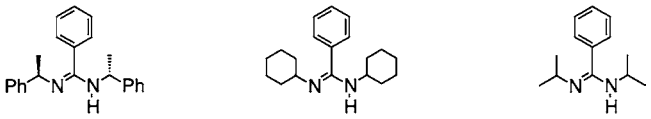

9.75 < 11.34 < 11.69

(20) In anhydrous $CHCl_3$ containing 0.3−1 wt % ethanol as stabilizer, the rate of the chain exchange process (k) of (*R*)-**5a**·**6a** was estimated to be 30.4 M^{-1} s^{-1} at 25 °C, which is 4.8 times larger than that estimated in $CDCl_3$ containing silver foil as stabilizer. The CD intensity of (*R*)-**5a**·**6a** in anhydrous $CHCl_3$, however, was exactly the same as that in $CDCl_3$, which indicates that ethanol most likely affects the duplex formation in a kinetic process, but not in a thermodynamic one.